Corrosion Resistant Chemical Vapor Deposited Coatings for SiC and Si_3N_4

by

David W. Graham

Thesis submitted to the faculty of the

Virginia Polytechnic Institute and State University

in partial fulfillment of the requirements for the degree of

Master of Science

in

Materials Science and Engineering

APPROVED:

Dr. Jesse J. Brown, Chairman

Dr. Ronald S. Gordon, Department Head

Dr. Deidre A. Hirschfeld

April 1993

Blacksburg, Virginia

Corrosion Resistant Chemical Vapor Deposited Coatings for SiC and Si_3N_4

by

David W. Graham

Dr. Jesse J. Brown, Chairman

Materials Science and Engineering

ABSTRACT

Silicon carbide and silicon nitride turbine engine components are susceptible to hot corrosion by molten sodium sulfate salts which are formed from impurities in the engine's fuel and air intake. Several oxide materials were identified which may be able to protect these components from corrosion and preserve their structural properties. Ta_2O_5 coatings were identified as one of the most promising candidates. Thermochemical calculations showed that the chemical vapor deposition(CVD) of tantalum oxide from O_2 and $TaCl_5$ precursors is thermodynamically feasible over a range of pressures, temperatures, and reactant concentrations. The deposition of Ta_2O_5 as a single phase is predicted in regions of excess oxygen, where the reaction is predicted to yield nearly 100% efficiency.

CVD experiments were carried out to deposit tantalum oxide films onto SiC substrates. Depending on the deposition conditions, a variety of coating morphologies have been produced, and conditions have been identified which produce dense, continuous Ta_2O_5 deposits. Preliminary corrosion tests on these coatings showed no apparent degradation of the CVD deposited tantalum oxide coatings.

The feasibility of depositing $ZrTiO_4$ as a coating material was also investigated based on thermochemical considerations. Since no data were available for this material, thermodynamic values were estimated. Thermochemical calculations indicated the chemical vapor deposition of zirconium titanate from O_2, $ZrCl_4$, and $TiCl_4$ occurs over a range of temperatures in a very narrow region of the phase diagram. Deviations from the single phase region predicted the codeposition of either ZrO_2 or TiO_2 with $ZrTiO_4$.

These results suggested that the chemical vapor deposition of $ZrTiO_4$ may be difficult from a process handling perspective. Additionally, the process is predicted to be very inefficient, leaving substantial amounts of unreacted chlorides in the reactor exhaust.

ACKNOWLEDGEMENTS

First and foremost, I must express my deepest appreciation and gratitude to Dr. Jesse Brown and Dr. Deidre Hirschfeld at Virginia Tech and David Stinton at Oak Ridge National Laboratory. They provided me not only with a graduate program which led to this work and the completion of my degree, but with a truly unique experience. I cannot even begin to enumerate the benefits of the time which I spent in Oak Ridge.

I also thank the members of my committee for their efforts: Dr. Ronald Gordon, Dr. Jesse J. Brown, and Dr. Deidre Hirschfeld.

I owe many, many thanks to those with whom I was able to work at Oak Ridge National Laboratory. They include Dave Stinton, Rick Lowden, Ted Besmann, Woo Lee, Jerry McLaughlin, Kevin Cooley, Millicent Clark, Laura Riester, Harry Livesy and Jane Lowe from the Ceramic Surface Systems Group; John White, Otto Schwarz, Norman Vaughn, Michael Stott, Jim Miller, Matt Walukas, Kristin Ploetz, Kim Bell, Cameka, and Subu from the assortment of co-ops; and Burl Cavin, Cam Hubbard, Dorothy Coffey, and the rest of the HTML User Center staff. During my stay in Oak Ridge, I also had the privelege of working with Bill Weaver of the 3M Corporation as well as Bernie Gallois of the Stevens Institute of Technology.

Of the students and staff at Virginia Tech, I must include Eric Wuchina, Bill Russ, Gary Pickrell, Tawei Sun, Yaping Yang, Susan Fleming, Katie Hutchinson, Laurie Dodge, and Jan Doran.

On a personal level, I cannot forget my friends and family. My sister and

especially my parents have encouraged me through every step of my graduate work. My closest friends - Carla Gilbert, Laura Harcum, Kim Fain, Carrie Gocolinski, Melissa Mellon, Kim Reinbold, Julie Handy, and Greg Super - will never know how much their support was truly appreciated and, at times, needed. I must also thank my roommates: Jeramie, Kim, Tom, Melanie, Matt, and James. My other family, the New Virginians, cannot escape recognition either. As individual members and as a whole, the New Virginians have provided me with not only with an outlet for my musical and technical skills, but they have truly been a family willing and able to give me support, and they have seen me grow and develop over the past few years. I only wish that the group could be around when I return to Tech in the future as an alumnus.

There are far too many reasons why I have included each and every name. Professional and work related reasons would only scratch the surface. Every person is well deserving of recognition - even if he or she simply let me blow off steam once in a while. Regardless, every one has been a part of my life over the past two years, and every one has helped me to enjoy the time I have spent in either Blacksburg or Oak Ridge. I honestly and sincerely thank you all from the bottom of my heart.

Finally, I must include the official credit line which acknowledges the financial support for my work:

Research sponsored by the U.S. Department of Energy, Assistant Secretary for Conservation and Renewable Energy, Office of Transportation Technologies, as part of the Ceramic Technology Project of the Materials Development Program, under contract DE-AC05-84OR21400 with Martin Marietta Energy Systems, Inc.

TABLE OF CONTENTS

LIST OF FIGURES

LIST OF TABLES

CHAPTER 1: INTRODUCTION

Oxide and nonoxide ceramics such as silica, alumina, nitrides, and carbides are finding increasing numbers of applications for use as structural components and electronic devices. The interest in ceramic materials can be attributed mainly to their high chemical and thermal stability, high strength to weight ratio, high hardness, excellent wear resistance, and a variety of other properties.[1-5]

Recent research efforts in the field of structural ceramics have mainly concentrated on the development of high performance ceramic components, including turbine blades, rocket nozzles, and parts for gas turbine engines, which are targeted for use in a variety of military and civil applications. At the same time, there has been a steady interest in developing advanced chemically vapor deposited ceramic films to be used as protective coatings, enhancing the performance and service life of many metallic and nonmetallic structural components.[5-11]

In recent years, comprehensive development of silicon carbide and silicon nitride materials has been underway to produce components for use in a wide variety of applications such as heat exchangers, hot gas cleanup systems, and advanced heat engines. These types of systems typically operate at elevated temperatures, and the atmospheres in which these materials are expected to perform are well known to contain highly reactive and possibly corrosive gases, particulates, and contaminants. Superior component performance in these environments demands that a material's stability, its

compatibility with other materials in the operating system, and its reactivity with likely or possible contaminants be considered.

In this study, the development of coatings to protect silicon carbide and silicon nitride components from corrosion is investigated. Candidate coating materials were first selected which would be able to protect components from corrosion. Using the ChemSage thermochemical equilibrium computer program, thermodynamic analyses were performed to evaluate processes by which Ta_2O_5 and $ZrTiO_4$ may be deposited by chemical vapor deposition. Deposition work was performed to produce Ta_2O_5 coatings and optimize their structure. Additionally, preliminary corrosion tests were carried out to evaluate the performance of the Ta_2O_5 coatings.

It should be noted that this text was originally written as three separate works. These three papers comprise the three separate chapters of this text.

CHAPTER 2: THERMODYNAMIC CONSIDERATIONS FOR THE DEVELOPMENT OF Ta_2O_5 CORROSION RESISTANT COATINGS

Introduction

In the past several decades, the world has witnessed the fluctuation and especially the increases in the cost of the production of fuels, which is influenced heavily by the cost of petroleum. More recently, the world's leaders have become increasingly concerned with the environmental consequences of living in an industrial society. Both of these factors have directed engineers and researchers toward the heavy interest which can now be found in the efforts to develop more efficient internal combustion engines. The achievement of significant increases in efficiency dictates that engines must operate at higher temperatures. The magnitude of the temperatures which are required is well above the operating limits for traditional metals. Even the metallic superalloys would not be capable of withstanding the combination of high temperature and high stresses which would be found in this environment.

In order to pursue the goal of more efficient engines, ceramics such as silicon carbide and silicon nitride have been developed for use as high temperature structural components in advanced gas turbine engines. As a result of the dramatic increase in

operating temperature, chemical reactions can proceed much more quickly towards completion. The speed at which these reactions can occur may lead to the production of corrosive products in the engine as well as enhance the corrosive reactions themselves. The effect of corrosion is the degradation of the ceramic surface and subsequently the mechanical properties of the components, which in turn leads to the failure of the engine.

Ta_2O_5 is being investigated for use as a coating to protect silicon carbide and silicon nitride heat engine components from corrosion. As in the selection of any material system, significant attention must be paid to the possibility of chemical interactions which may occur. At reasonably high temperatures, chemical reactions can proceed very rapidly, reaching equilibrium in a short amount of time. A thermodynamic analysis of the material system under consideration provides important information about the chemical compatibility of a coating material with its environment. Additionally, thermochemical modeling has been shown to be essential in analyzing the potential which may exist for a chemical vapor deposition process. A short analysis and review of the phase equilibria between the SiC and Si_3N_4 engine components and their environment is first presented. The utility of tantalum oxide coatings is then evaluated with respect to the compatibility of Ta_2O_5 with SiC, Si_3N_4, and the corrosive environment in which they would perform. Finally, thermodynamic equilibrium calculations are used to evaluate the production of Ta_2O_5 coatings by chemical vapor deposition.

Thermochemical Analysis

The ChemSage computer program[12] was used to calculate chemical equilibria. This program uses numerical techniques to minimize the total Gibbs free energy of all of the possible gaseous, liquid, and solid species which may be present in a particular chemical system. As with all computer programs, the results which may be obtained from these calculations are only as good as the data which are input into the routine. In

thermochemical calculations, the accuracy of the results will depend upon two factors in particular: the inclusion and omission of chemical species for consideration in equilibrium calculations, and the accuracy of the thermodynamic data which are utilized for these calculations.

Accompanying the ChemSage program was the thermodynamic database developed by Scientific Group Thermodata Europe (SGTE)[13] and the Microtherm[14] databank management computer program. In the SGTE database, thermodynamic data are compiled in terms of the standard enthalpy of formation, ΔH°_f, at 298.15K, the entropy S° at 298.15K, the standard enthalpy of transformation ΔH° for phase transitions, and the molar specific heat at constant pressure C_p. The data for heat capacity are expressed as a function of temperature T so that $C_p = a + bT + cT^2 + dT^{-2}$ where a, b, c, and d are constants and T is in Kelvin. In addition to supplying database management capabilities, the Microtherm program also provided for the computation of various thermodynamic quantities such as the standard free energy of formation, ΔG°_f.

The standard free energies of formation at 298.15K and 1600K of the chemical species considered in the system Ta-O-Cl-Si-C-N-Na-S-H are enumerated in the appendix. Solid, liquid, and gaseous species are denoted with (s), (l), and (g), respectively; condensible species are noted with (c), indicating the presence of either a solid or liquid, depending on the temperature. These values were calculated from thermodynamic data by the Microtherm program. To ensure the accuracy and integrity of the data contained in the SGTE database, the values for ΔG°_f were compared to recent modifications in the JANAF Tables[15] as well as to data compiled by Barin[16]. Although minor variations in data were encountered, the overall agreement between the three databases was good. Only a few of the species had values of ΔG°_f which differed between the databases by more than 2 kJ/mole. The chemical equilibria for this system is expected to be insensitive to such minor variations due to the magnitude of the energies of formation of the compounds in this system which are expected to be stable.

Discrepancies did exist, however, which must be addressed. Of primary

importance were discrepancies in the data for the reference states of Na and S, as data from the reference state are used to calculate the free energy of formation of all of the chemical species. In the SGTE database, the data for Na(c) are used as the reference state. As a result, only data for the solid and liquid phases up to temperatures of 1200K are included. To ensure agreement with the more complete reference state data found in the JANAF tables, the liquid to gas transformation at 1170K was added and heat capacity data was entered into the database to extend the validity of the data to 2000K. The JANAF tables - as well as Barin's data, which were largely derived from these tables - arbitrarily chose the reference state of sulfur in the gas phase as 0.5 S_2(g) above 882K. The data in the SGTE database were altered to reflect this standard, adding the liquid to gas transformation at 882K and modifying the heat capacity data to increase the temperature limit of the data to 2000K.

After the modifications were made to the sodium and sulfur data, discrepancies were still found between the SGTE database, the JANAF tables, and Barin's compiled data. The data for CCl_4(l) and CCl_4(g) were modified to reflect the more recent enthalpy and entropy data found in Barin. The enthalpy of Ta_2C(s), the entropy data for TaN(c) and Ta_2N(c), and enthalpy, entropy, and heat capacity data for Ta_2Si(s) and Ta_5Si_3(s) were all updated to the data found in Barin. The temperature limits of NaO_2(s) and Na_2S_3(c) were extended to 2000K and 1000K, respectively. For α-Si_3N_4, Na_2(g), Na_2S(c), S_3(g), S_4(g), S_5(g), S_6(g), S_7(g), and S_8(g) all of the thermodynamic data for each species was modified to reflect more recent and accurate data found in the JANAF tables.

To improve not only the accuracy but the completeness of the database, species for which data could be found in either the JANAF tables or in Barin's data but which were not already a part of the SGTE database were also considered for the calculations. As a result, the thermodynamic data for TaS_2(s), TaS(g), Si_2Ta(s), TaCl(g), $TaCl_2$(g), Na_2SO_3(c), Na_2S_4(c), $NaNO_3$(c), $NaNO_2$(c), SiH_3Cl(g), $NaClO_4$(s), SCl_2(l), N_2H_4(l), Na_2S_2(c), N_2O_5(g), C_2H_3Cl(g), C_2H_5Cl(g), CH_2O_2(g), $SiCH_3Cl_3$(g), $Si(CH_3)_4$(g), and

$C_2Cl_6(g)$ were added to the database.

Thermochemical Stability of SiC and Si_3N_4 in the Engine Environment

The hostile environment of a gas turbine engine has generated much interest in the corrosion behavior of SiC and Si_3N_4. Extensive work has already been performed on the corrosion of these materials by Na_2SO_4.[17-31] An excellent review of this work is contained in the paper by Fox *et al.*,[18] who asserted that NaCl ingested in the engine from the intake air or sodium impurities in the fuel would react with sulfur impurities in the fuel and proposed the following reaction for the formation of sodium sulfate:

$$2\ NaCl(s) + SO_3(g) + H_2O(g) = Na_2SO_4(l) + 2\ HCl(g)$$

As these products travel down the hot-gas-path of the engine, sodium sulfate condenses onto components at temperatures below its dew point. Hot corrosion of the turbine engine is then possible when the liquid salt is in contact with the components.

Silicon-based ceramics oxidize at high temperatures and form a layer of silica which protects the material from further oxidation.[18,32] The production of the native oxide layer occurs via the following reactions for silicon carbide and silicon nitride, respectively:

$$2\ SiC(s) + 3\ O_2(g) = 2\ SiO_2(s) + 2\ CO(g)$$
$$Si_3N_4(s) + 3\ O_2(g) = 3\ SiO_2(s) + 2\ N_2(g)$$

Hot corrosion of silicon based ceramics occurs by the dissolution of the silica layer to form a non-protective liquid product[18-21,33] in the reaction:

$$x\ SiO_2(s) + Na_2SO_4(l) = x\ SiO_2(s) + Na_2O(s) + SO_3(g) = Na_2O \cdot xSiO_2(l) + SO_3(g)$$

In this reaction, the formation of the sodium silicate liquid is governed by the activity of Na_2O, which is controlled in turn by the partial pressure of SO_3. At 1000°C, partial pressures of SO_3 greater than 0.1 Pa (10^{-6} atm.)[18,19] reduce the activity of Na_2O to less than 10^{-10} and inhibit the reaction between silica and sodium sulfate from taking place. In engines using high-purity fuels, however, calculations have shown SO_3 levels to be quite low,[18,19] allowing the dissolution reaction to proceed.

Once the protective silica layer has been removed from the surface of the component, degradation of the component material itself may begin. Because of the competing processes of continuing oxidation and corrosion by sodium sulfate at high temperatures, an exact determination of the mechanisms by which the mechanical properties of the materials degrade is difficult. Irrespective of the exact mechanism of attack, silicon carbide undergoes extensive pitting of the exposed surface as a result of the attack, and silicon nitride suffers attack of the oxide grain boundary phases, leading to the degradation of mechanical properties.

In the reaction in which sodium sulfate is formed, HCl is also produced in the engine. Computations of thermodynamic equilibrium provide insight into the possibility of reactions which may occur with HCl. As shown in Figure 2.1, a mixture of one mole of HCl and one mole of SiC undergoes only a slight reaction. At high temperatures, only approximately fifteen percent of the SiC decomposes to form free carbon and minor amounts of silicon chlorides. The small extent of the reaction with SiC suggests that SiC might be stable with respect to HCl because of the lack of a substantial thermodynamic driving force for the reaction to decompose silicon carbide. The interaction of HCl with silicon nitride is illustrated in Figure 2.2. This diagram shows that silicon nitride is even more stable than SiC in an environment containing HCl, as almost no reaction occurs with silicon nitride. The interactions between HCl and silicon carbide and silicon nitride have also been studied experimentally.[34-38] For silicon carbide and HCl at 950°C, essentially no reaction was observed. This was attributed to the difficulty in dissociating HCl at high temperatures.[35] Only very slight degradation occured in silicon nitride

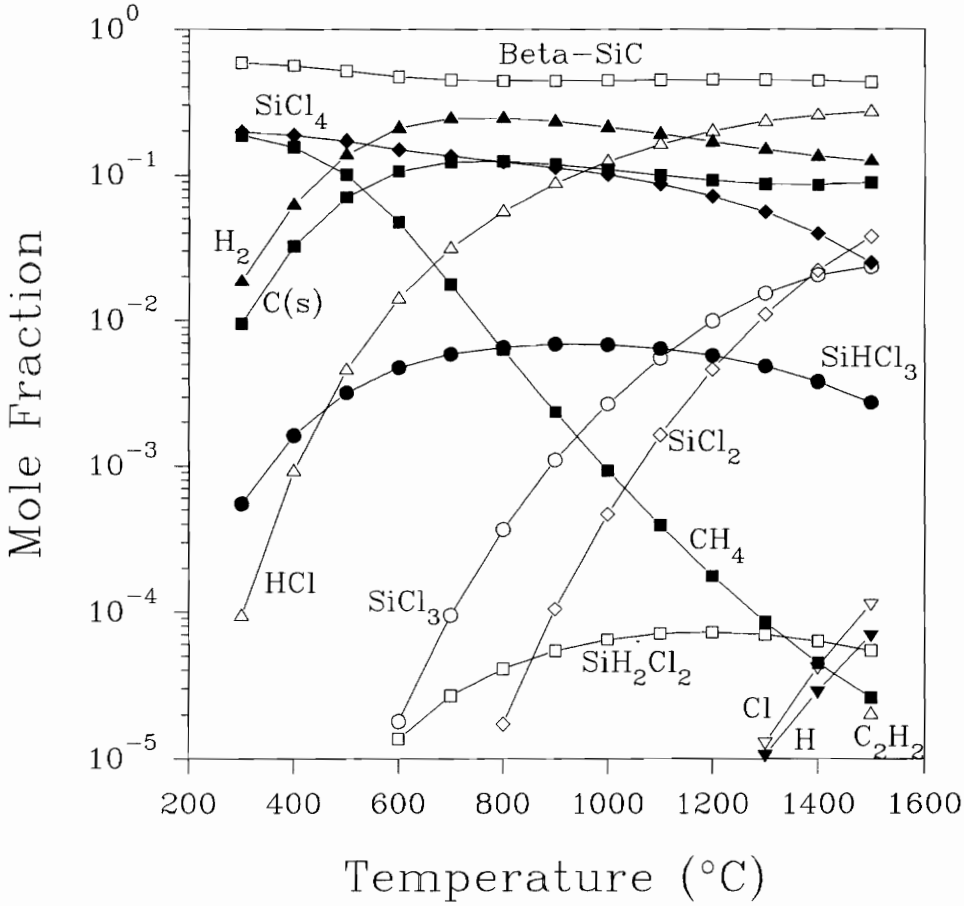

Figure 2.1: Equilibrium composition of a mixture of 1 mole SiC and 1 mole HCl at 101kPa

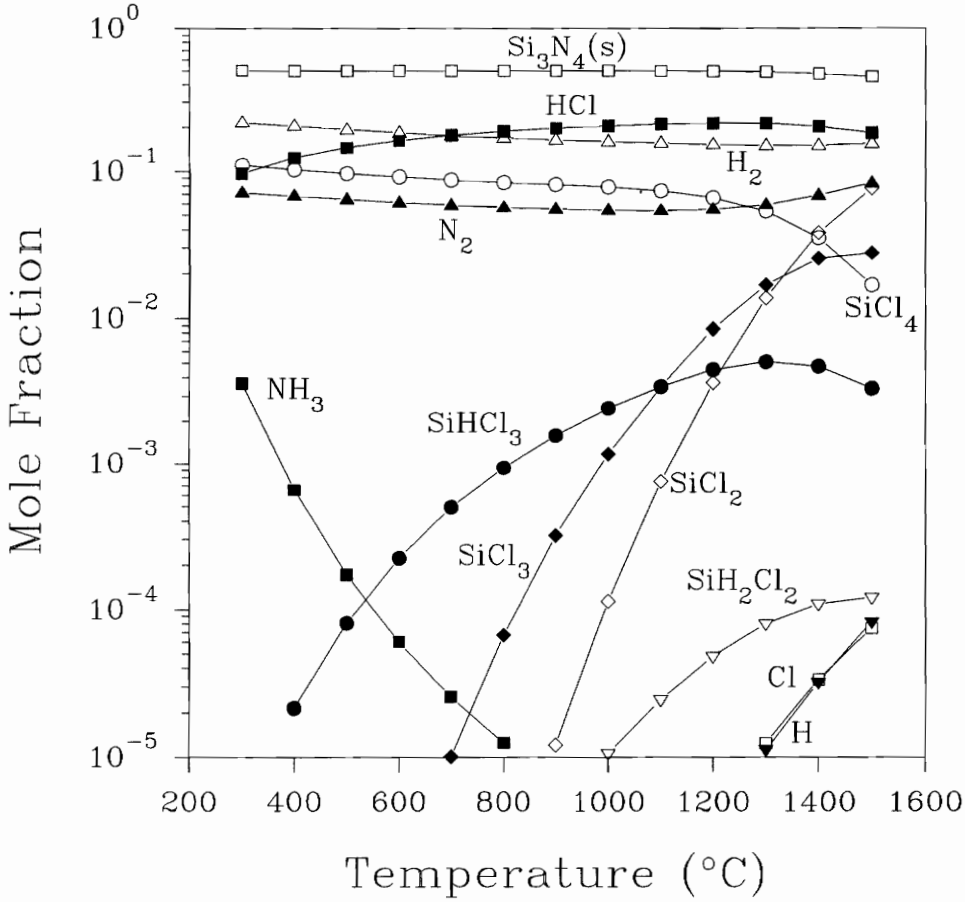

Figure 2.2: Equilibrium composition of a mixture of 1 mole Si_3N_4 and 1 mole HCl at 101 kPa

materials. In this case, HCl reacted with the oxide grain boundary phases, dissolving the cations, but dissolution of silicon from the matrix was negligible. As is the case with sodium sulfate, the protective layer of SiO_2 must first be penetrated before corrosion of the ceramic component can begin. Lin[39] reported that in HCl/N_2 mixtures at low pressures, the reaction of SiO_2 with HCl produces $SiCl_3$ and $SiCl_2$ as the major reaction products in the gas phase at temperatures above 1250°C, while no reaction occurs at lower temperatures. However, these products were only present in very small amounts. Again, as with SiC and Si_3N_4, the extent of the reaction was very small. As shown in Figure 2.3, thermochemical computations support those findings. In a mixture containing one mole each of HCl and SiO_2 at 101 kPa, only slight decomposition of the silica is expected if the reactants are allowed to continue to react until equilibrium is reached.

Obviously, the work which has been done to date indicates that silicon carbide and silicon nitride turbine engine components will not survive in their operating environment. The slow erosion of the protective silica coating by HCl could, in sufficient time, expose components to oxidation. However, the effect of HCl corrosion is made negligible by the much faster rates of corrosion of both the silica and the component by sodium sulfate. Indeed, the components of gas turbine engines must be protected from their operating environment.

Thermochemical Stability of Ta_2O_5 in the Engine Environment

An additional need for the protective silica coating on silicon nitride and silicon carbide is demonstrated in Figures 2.4 and 2.5 respectively. These are calculated diagrams of the equilibrium condensed phases in the systems Ta_2O_5 - Si_3N_4 and Ta_2O_5 - SiC, respectively. In Figure 2.4, it can be seen that tantalum oxide and silicon nitride are unstable as a material couple. At all compositions except 46.5% silicon nitride and at all temperatures, the equilibrium composition of the system involves the complete

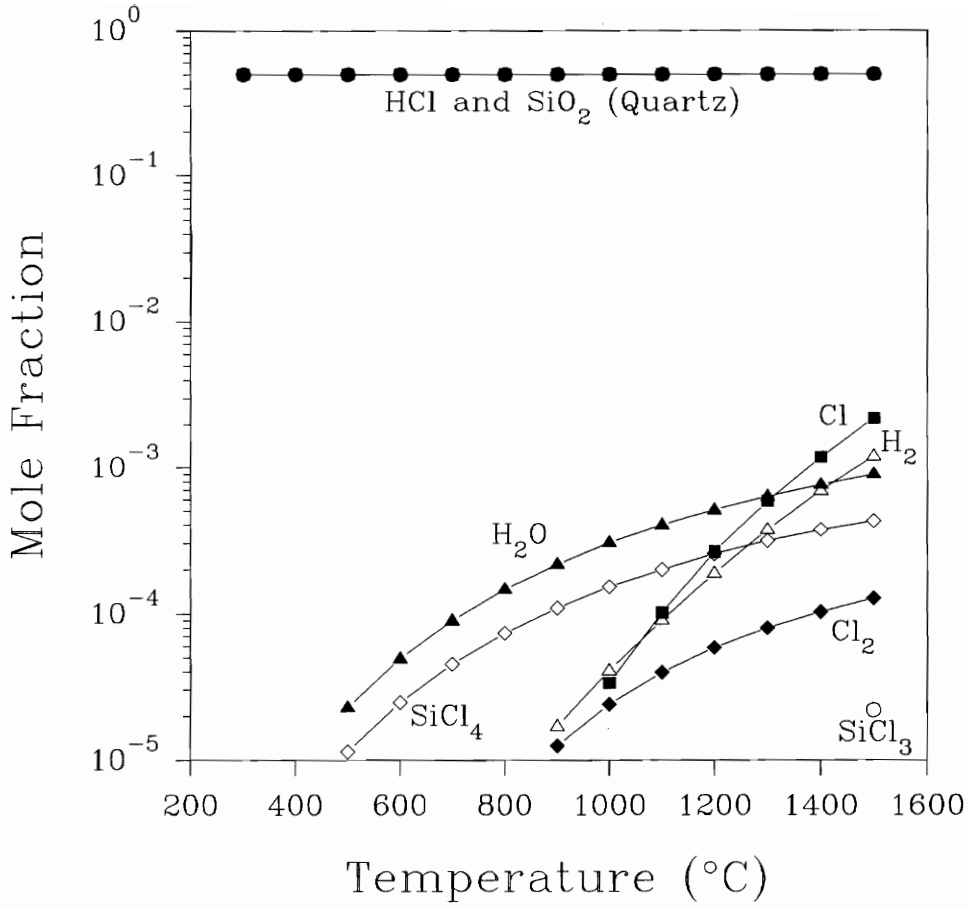

Figure 2.3: Equilibrium composition of a mixture of 1 mole SiO_2 and 1 mole HCl at 101 kPa

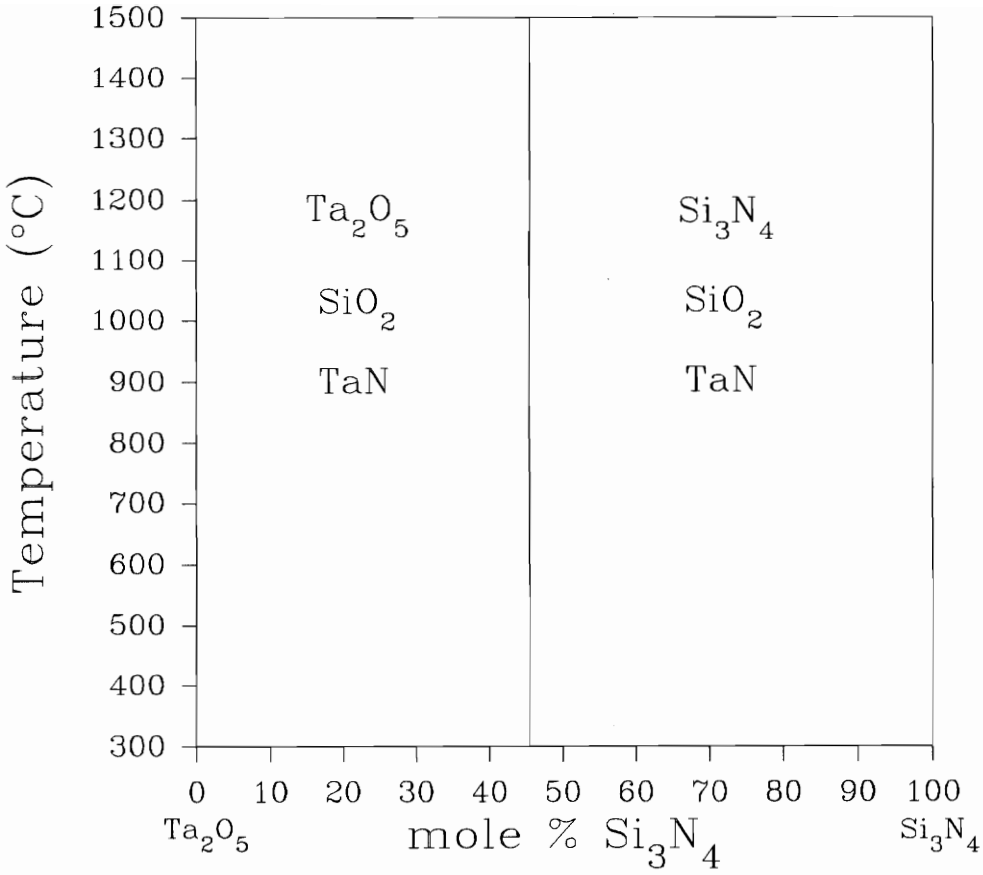

Figure 2.4: Calculated phase diagram of the system Ta_2O_5 - Si_3N_4

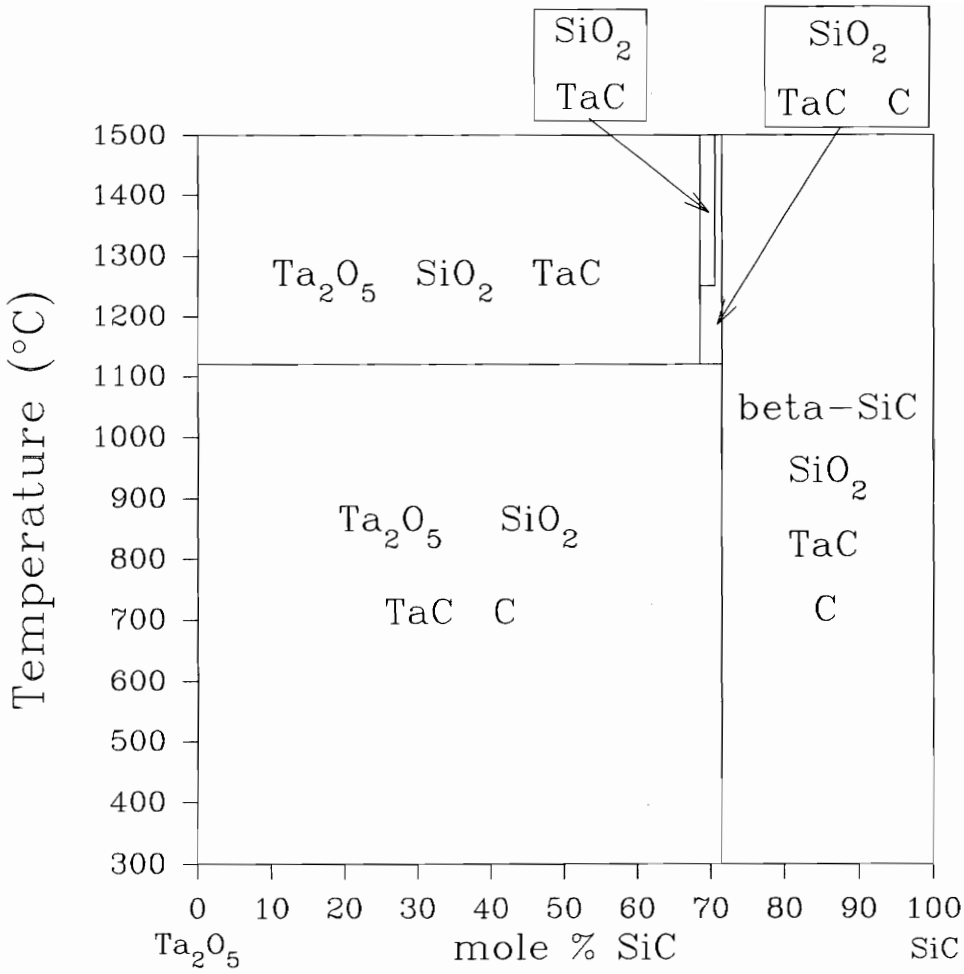

Figure 2.5: Calculated phase diagram of the system Ta_2O_5 - SiC

decomposition of either tantalum oxide or silicon nitride to produce silica and tantalum nitride. Similar results may be found for the tantalum oxide - silicon carbide system, as shown in Figure 2.5. In this case, the decomposition reactions form silica, tantalum carbide, and, except in the tantalum oxide rich regions at temperatures above 1120°C, free carbon. While this diagram is slightly more complex than that involving silicon nitride, it also illustrates that total decomposition of one of the phases is predicted. Thus in each of these systems, thermodynamic calculations suggest that the silica layer may be needed as a protective coating to prevent the degradation of both the tantalum oxide coating and the silicon nitride or silicon carbide substrate beneath it.

Because of the native layer of silica which forms on silicon based ceramics, the bonding of a coating material to an engine component will occur between the silica and the coating. Thus the chemical compatibility of silica with any coating material must be investigated. Although qualitative phase diagrams may be found,[40] phase equilibria for the silica - tantalum oxide system do not appear to be well established. These studies indicate the formation of several phases of intermediate composition and a liquidus of 1550°C. Because typical engine component temperatures in the region where corrosion is expected are approximately 200 to 400°C below this liquidus temperature, it is expected that solid state reactions are unlikely. The addition of silica to tantalum oxide forms intermediate phases which were structurally quite similar to the Ta_2O_5 structure,[40] indicating that these materials may be structurally compatible and the formation of intermediate phases would not necessarily be catastrophic to the Ta_2O_5 coating's adherence or its performance. This conclusion appears to be supported by the work of others. In the chemical vapor deposition of Ta_2O_5 coatings on Si substrates, Takahashi and Itoh[41] found that $TaSi_2$ could be formed along with Ta_2O_5 depending on the experimental conditions. Even in the presence of $TaSi_2$ deposits, uniform, adherent coatings were produced and no problems with material compatibility were reported. In the chemical vapor deposition of Ta_2O_5 coatings on both SiO_2 and Si_3N_4 substrates by Kaplan *et al.*,[42] no phases other than Ta_2O_5 were found, even after annealing the

coatings. Thus in this work, no chemical interactions were found between Ta_2O_5 and either SiO_2 or Si_3N_4.

The phase diagram of the Ta_2O_5 - Na_2O system shows that no liquid phases exist below 1625°C.[43] In this case, typical turbine engine component temperatures are 300 to 500°C below the liquidus temperature, making the formation of any sodium tantalate phases seem unlikely. Thermochemical computations were used to consider the possibility of reaction between Ta_2O_5 and HCl. As shown in Figure 2.6, the equilibrium composition of one mole of Ta_2O_5 and one mole of HCl would undergo slight decomposition at elevated temperatures. In the dynamic environment of a turbine engine, however, gases are moving at high velocities through the engine, creating a regime in which reactions must proceed very quickly if equilibrium is to be achieved. Considering the additional difficulty in dissociating HCl at high temperatures,[35] it is unlikely that any reaction would be allowed to occur between HCl and Ta_2O_5.

Chemical Vapor Deposition of Ta_2O_5

The reactor design for the deposition of Ta_2O_5 requires the analysis of two separate reactions. In the first stage of the reactor, chlorine gas is passed over tantalum wire at elevated temperatures to produce $TaCl_5$. O_2 is then introduced into the reactor by a separate inlet. In the second stage of the reactor, these gases flow into the hot zone and react to deposit Ta_2O_5.

The first step in evaluating a CVD process involves examining the reactivity and volatility of the precursors in order to determine their transportability and chemical integrity as reactants at high temperatures. Lee *et al.*[44] recently demonstrated the need for this type of examination when discovering that it is crucial to understand the decomposition characteristics of NH_3 before a competent analysis of the thermodynamics of the chemical vapor deposition of Si_3N_4 from SiF_4 and NH_3 can be correctly performed.

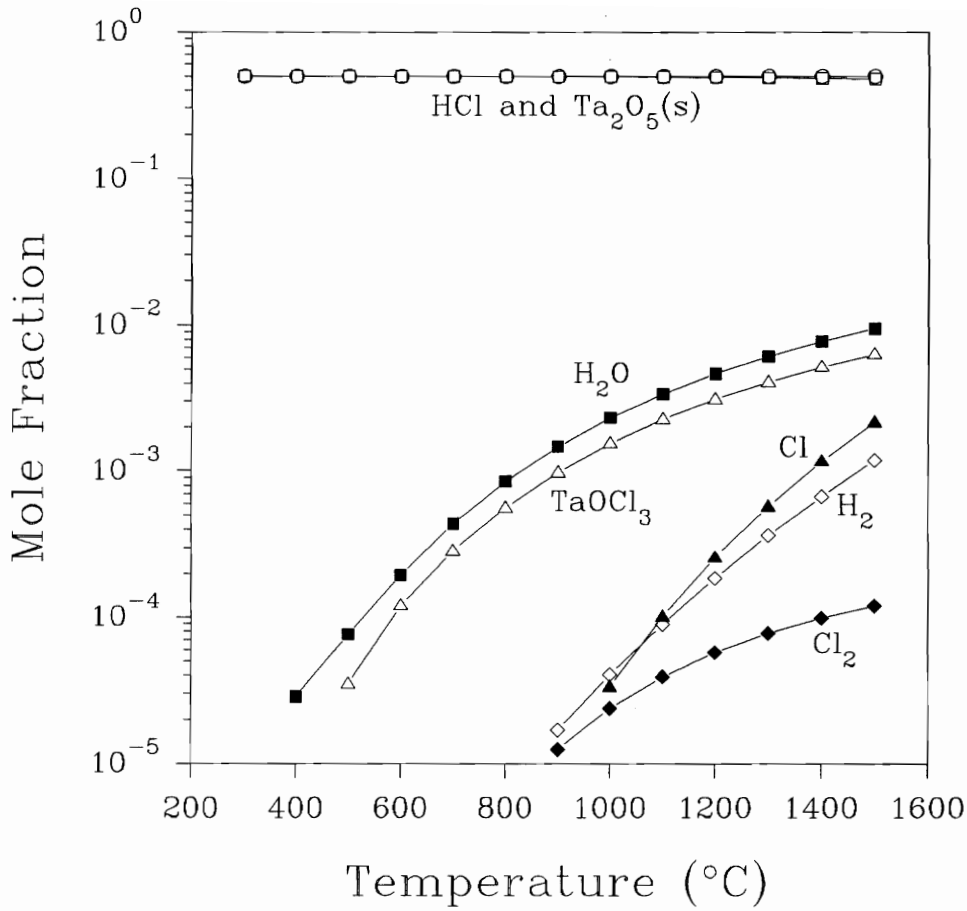

Figure 2.6: Equilibrium composition of a mixture of 1 mole Ta_2O_5 and 1 mole HCl at 101 kPa

Considering the chlorination of tantalum at atmospheric pressure, the equilibrium composition that is expected for the thermal decomposition of $TaCl_5$ is shown in Figure 2.7. This figure shows that $TaCl_5$ is quite stable up to 1500°C, with only small amounts of $TaCl_4$, Cl, and Cl_2 being formed at higher temperatures. As shown in Figure 2.8, the equilibrium composition of $TaCl_5$ at 6.67 kPa (50 Torr) indicates that tantalum pentachloride is relatively stable at reduced pressures as well. In this case, approximately 30% of $TaCl_5$ decomposes to form $TaCl_4$ and Cl at 1500°C. The other chlorides such as TaCl, $TaCl_2$, and $TaCl_3$ are unstable in temperature and pressure ranges studied. These calculations show that $TaCl_5$ would be stable and acceptable for consideration as a precursor within a wide variety of temperature and pressure regimes. In the production of $TaCl_5$, Takahashi and Itoh[41] recommended its formation by reacting Cl_2 with tantalum metal at 600°C.

Thermochemical calculations can also be used to explore ranges of input parameters for a CVD system which will produce a specific condensed phase at equilibrium. A convenient method for displaying this information is the CVD phase diagram.[45,46] As in conventional phase diagrams, temperature, pressure, and composition may make up the axes which describe the parameters under consideration. These diagrams are plots of computed phase boundaries where the phase regions indicate the specific condensed phases which are the equilibrium products.

Figure 2.9 is a CVD phase diagram constructed for the Ta-O-Cl system as a function of temperature and the molar ratio $TaCl_5/(O_2+TaCl_5)$ at a pressure of 6.67 kPa. As can be seen in the diagram, Ta_2O_5 is thermodynamically favored to be deposited as a single phase under excess O_2 conditions over the entire temperature range of 300 to 1500°C. The reaction of $TaCl_5$ and O_2 to produce Ta_2O_5 is nearly 100% efficient in the region of excess oxygen as shown in Figure 2.10. Additionally, this figure demonstrates that under conditions of excess oxygen, $TaCl_5$, as well as the other tantalum chlorides, are unstable in the gas phase. In the region of no solid deposition, tantalum chlorides and $TaOCl_3$(g) are stable as shown in Figure 2.11. When reactor pressure is increased

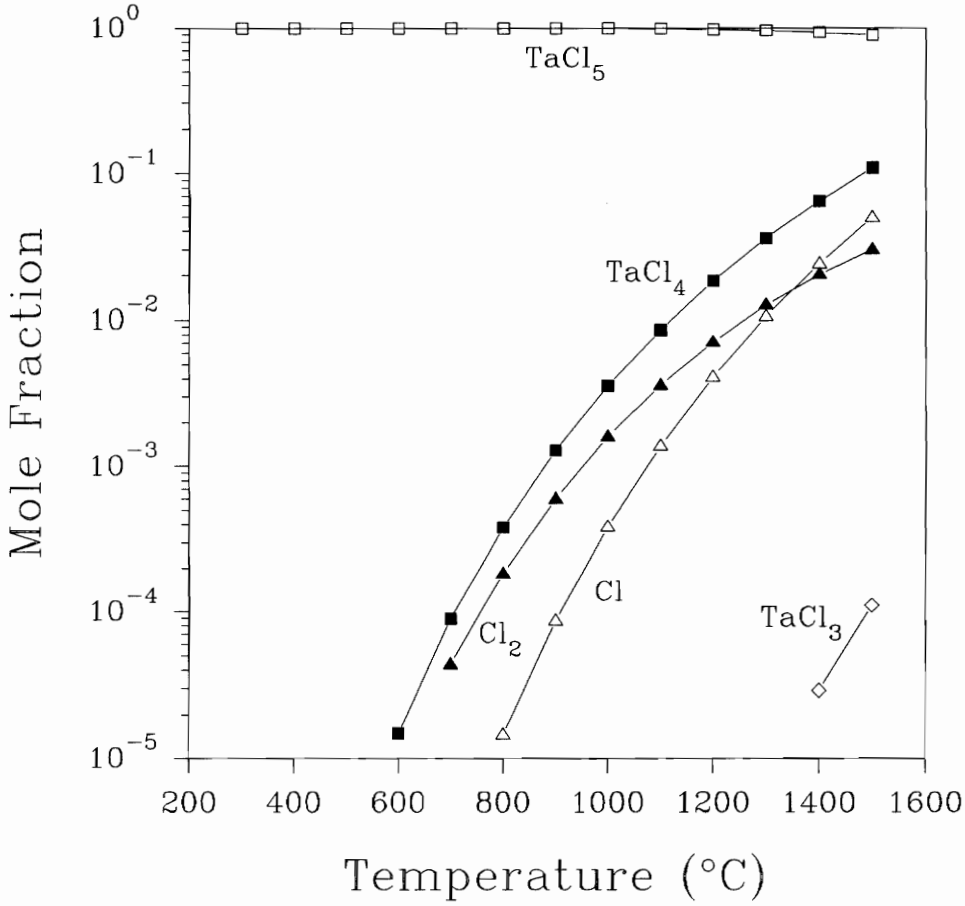

Figure 2.7: Equilibrium composition of 1 mole $TaCl_5$ at 101 kPa

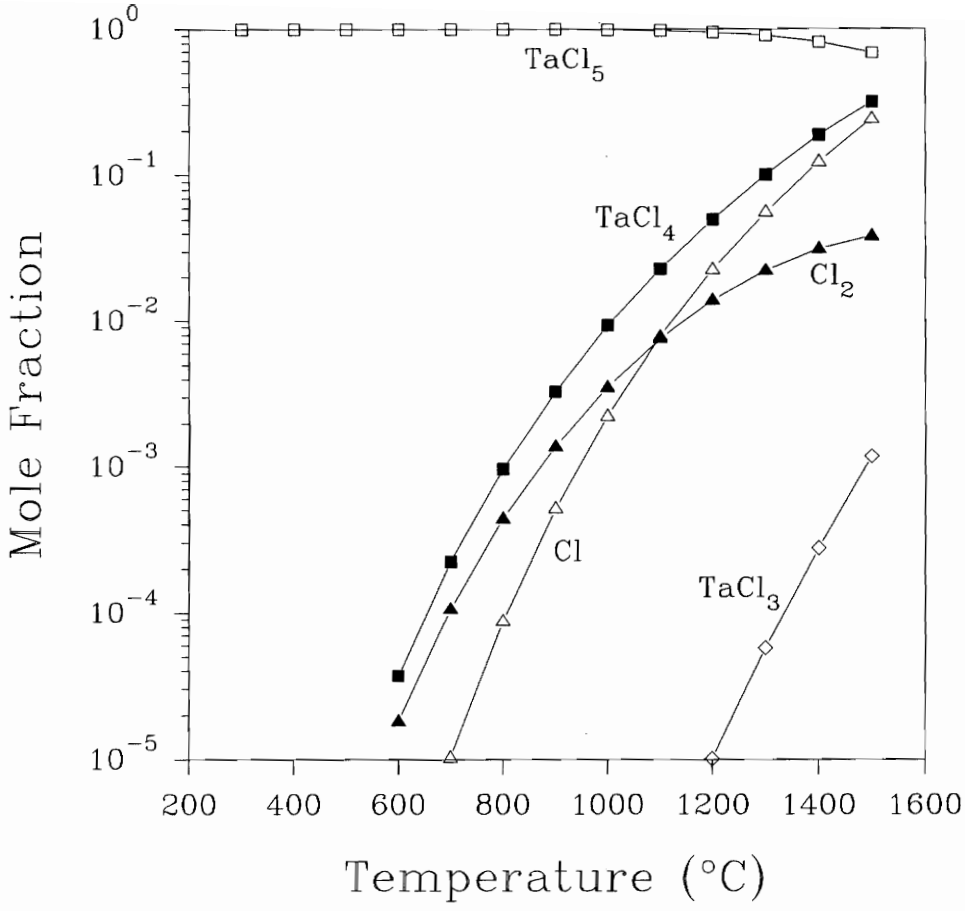

Figure 2.8: Equilibrium composition of 1 mole $TaCl_5$ at 6.67 kPa

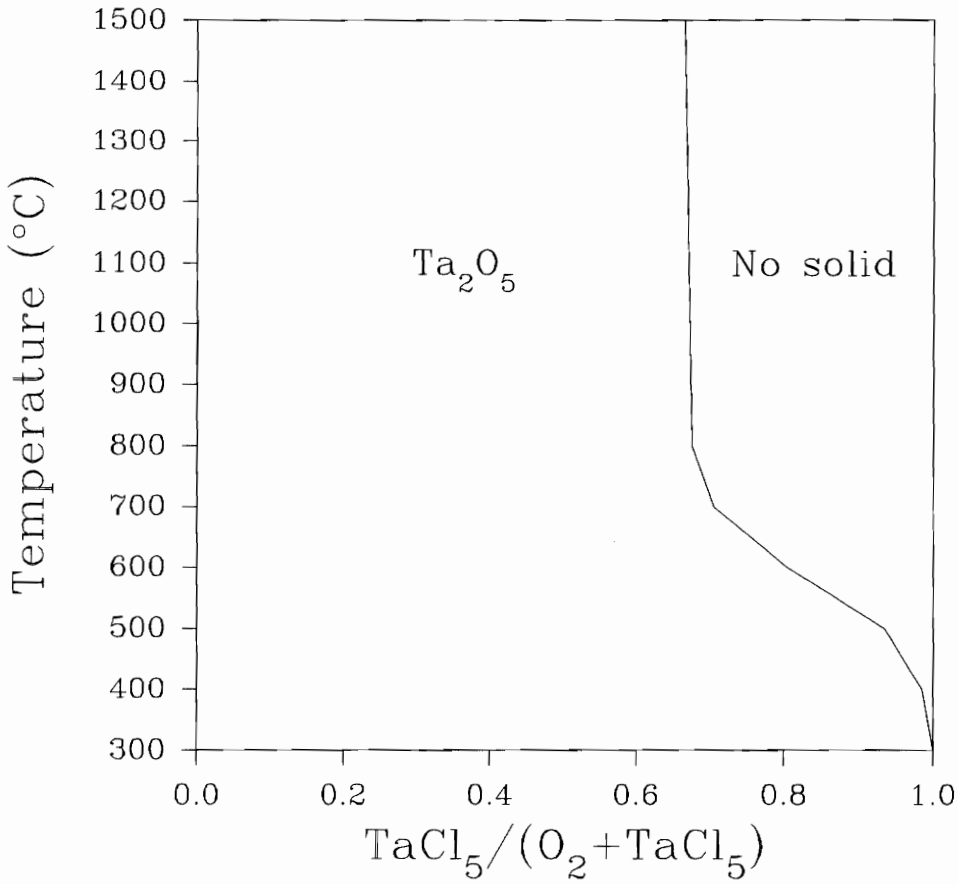

Figure 2.9: CVD phase diagram for the Ta-O-Cl system calculated at 6.67 kPa

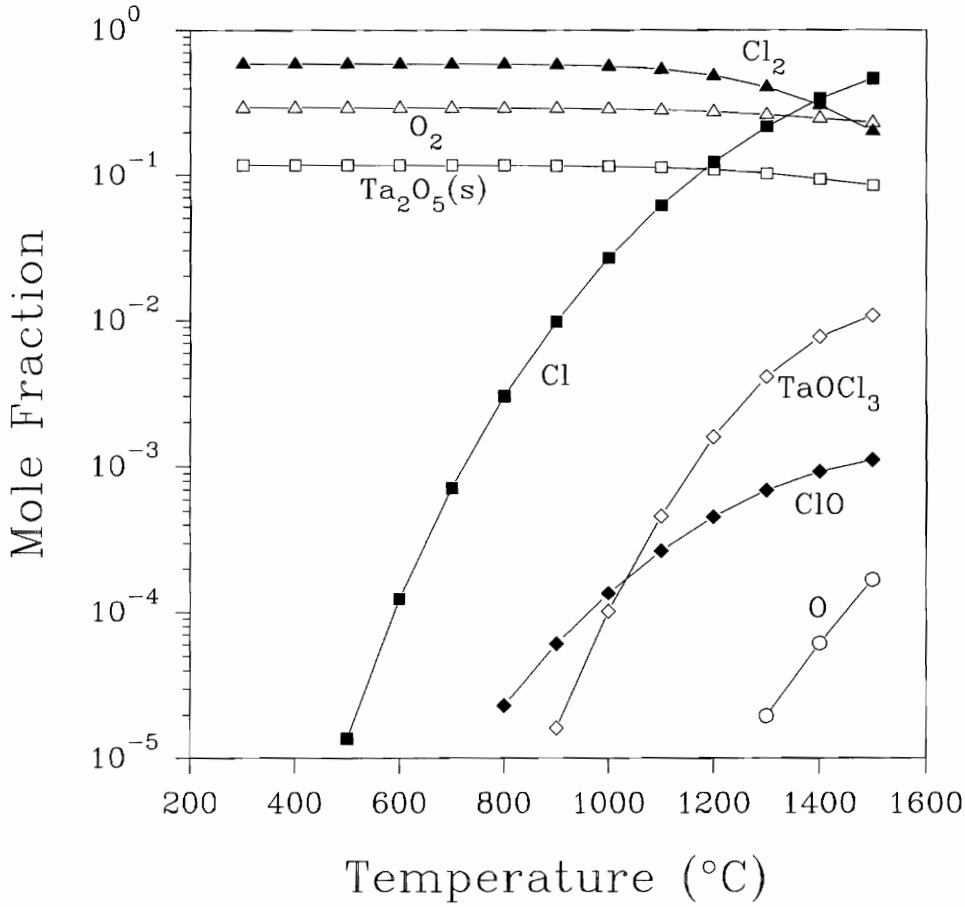

Figure 2.10: Equilibrium composition of a mixture containing 2 moles $TaCl_5$ and 5 moles O_2 at 6.67 kPa

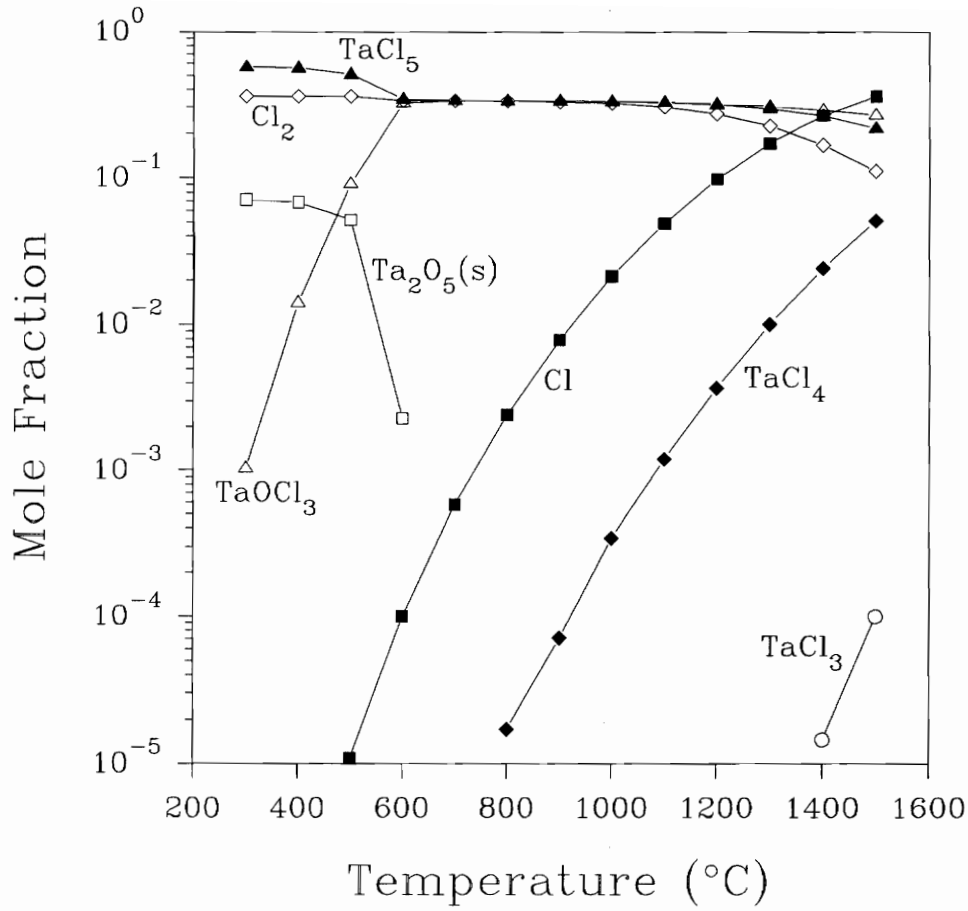

Figure 2.11: Equilibrium composition of a mixture containing 4 moles $TaCl_5$ and 1 mole O_2 at 6.67 kPa

to 101 kPa, essentially the same CVD phase diagram is generated. At increased pressures, the area of the region of no solid deposition decreases in size significantly at temperatures below 800°C.

Conclusions

Despite the results of phase equilibria studies and thermochemical equilibrium calculations, knowledge of the dynamic conditions which exist in a gas turbine engine combined with the data of previous workers indicate that Ta_2O_5 coatings may be suitable for the protection of engine components from corrosion by sodium sulfate. The chemical vapor deposition of Ta_2O_5 from O_2 and $TaCl_5$ is thermodynamically feasible over a range of presures, temperatures, and reactant concentrations. The deposition of Ta_2O_5 as a single phase is predicted in regions of excess oxygen, where the reaction is predicted to yield nearly 100% efficiency.

CHAPTER 3: CHEMICAL VAPOR DEPOSITION OF Ta_2O_5 CORROSION RESISTANT COATINGS

Introduction

Silicon carbide and silicon nitride materials have undergone extensive development in recent years for use in a wide variety of applications such as heat exchangers, hot gas cleanup systems, and advanced heat engines. In these types of systems, ceramics will be susceptible to hot corrosion in the form of attack by molten salts such as Na_2SO_4 formed from NaCl present in the atmosphere and sulfur impurities in the fuel.[30] Long term exposure to these types of conditions has been shown to degrade the properties of structural ceramics.[17,19,25,27,30]

Exposed surfaces of silicon-based ceramics oxidize at high temperatures to form a layer of silica which serves to inhibit further oxidation of the ceramic.[32] As described by others,[19-21,33] this silica layer can react with the molten salt to form a sodium-silicate liquid phase at temperatures above approximately 800°C, the eutectic temperature in the sodium-silica system.[47] As a result, the ceramic loses its protective layer and degradation of the ceramic occurs.[20,21,27]

Due to the nature of the service conditions under which these ceramic components are expected to perform, it becomes necessary to protect them from corrosion. Coatings are currently being developed which may protect SiC and Si_3N_4 components from salt-

induced corrosion.

Background

In 1986, GTE Laboratories initiated a program to develop a coating system which would protect SiC and Si_3N_4 heat engine components from both corrosion and contact stress damage. The development of such coatings is difficult because a mismatch between the coefficient of thermal expansion (CTE) of the coating and that of the substrate can cause the coating to crack or spall. To resolve this problem, the coating system shown in Figure 3.1 was developed by GTE to accommodate the stresses caused by the difference in CTE.[48,49] Initially, an AlN coating was deposited onto the substrates. During the chemical vapor deposition (CVD) process, chemical interactions produced a SiAlON-type compound which provided adherence to the substrate. The coating was then compositionally graded from AlN to $Al_xO_yN_z$ to Al_2O_3 + ZrO_2. Due to the absence of sharp interfaces and the gradual increase in thermal expansion from the interface to the outer Al_2O_3 + ZrO_2 protective coating, residual stresses in the coating were minimized, providing a coating system which should survive in the thermal environment found in heat engines.

GTE Laboratories' coating system seemed appealing for several years.[50,51] However, thermal cycling of their coatings produced cracks, severely degrading their ability to protect components from oxidation. As a result, the developers of this coating system concluded that the difference in thermal expansion between SiC or Si_3N_4 and the Al_2O_3 + ZrO_2 coating is too great to develop an adherent, crack-free coating.[50,51]

When considering additional materials which may be able to provide corrosion protection, several criteria must be established. The first and most obvious requirement is the ability of the coating to resist reaction with an aggressive salt layer. It must also have a CTE that is much closer to that of SiC and Si_3N_4. More closely matched CTE's

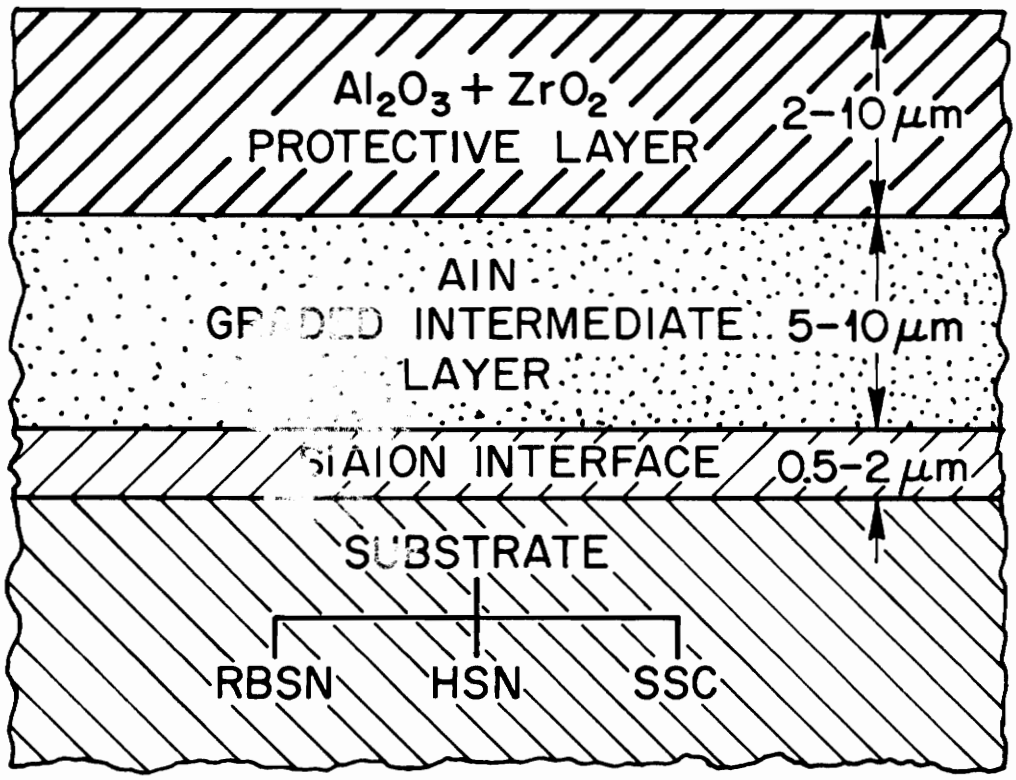

Figure 3.1: GTE's protective coating system

would overcome the problem of adherence as well as minimize noncatastrophic cracking which could allow molten salt to penetrate the coating and result in a loss of corrosion protection. The material must also be a stable oxide. This requirement will make the coating inherently oxidation resistant. Additionally, considerations for weight and cost must also be taken into account.

Carbon/carbon composites are well known to have potential for use in the aerospace industry. In these high temperature applications, however, they must be protected from oxidation. These composites are also known to have very low thermal expansion coefficients. As a result, after twenty years of investigation, no oxidation resistant coatings have been found that are capable of surviving the dramatic thermal cycles typical of aerospace environments. These investigations did, however, identify several materials with low CTE's that could be useful as coatings to protect SiC and Si_3N_4.[9,52-55] These materials are listed in Table 3.1.

$3Al_2O_3 \cdot 2SiO_2$ (mullite) is a material that has a CTE very close to that of SiC and it has performed reasonably well in corrosion tests, corroding somewhat more severely than Al_2O_3 but surviving significantly better than SiC.[17] Mullite's corrosion resistance is dependent on the absence of free SiO_2, which is readily attacked by sodium-containing salts.[20,21,27] Because of its corrosion resistance and low CTE, mullite is currently being investigated as a material for high temperature cross-flow filters that are exposed to sodium contaminants.[56]

Al_2TiO_5 also has a CTE that is quite low. It is currently being investigated as a protective coating for carbon/carbon composites and as a corrosion resistant material for turbine engine components.[57] Problems, however, do exist for this material. Its CTE is well known to be very anisotropic, causing significant microcracking in monolithic structures.[58] As with GTE Laboratories' coating system, this would obviously destroy the integrity of the coating and allow both oxygen and sodium salts to attack the components which it is designed to protect. Additionally, Al_2TiO_5 tends to absorb water and could degrade significantly if it were exposed to an environment containing small

Table 3.1

Refractory Oxides with Potential for Oxidation/Corrosion Protection

Compound	Density (g/cm^3)	CTE ($x10^{-6}/°C$)
Al_2O_3 *	3.97	8.0
$3Al_2O_3 \cdot 2SiO_2$	2.8	5.7
SiC *	3.21	5.5
$ZrTiO_4$	≈5	≈4
$HfTiO_4$	≈5	≈4
$Ta_2O_5 \cdot 6ZrO_2$	≈6	≈4
$Ta_2O_5 \cdot 6HfO_2$	≈6	≈4
Ta_2O_5	8.02	3.6
Si_3N_4 *	3.19	3.0
Al_2TiO_5	3.68	2.2
Carbon/carbon *	1.9	≈0

* Included only as a reference and not as a potential coating

amounts of moisture at high temperatures.

A number of investigations have shown the CTE of $ZrTiO_4$ to be quite low.[55,57,59-61] While the data summarized by Levin and McMurdie[62] show that $ZrTiO_4$ is thought to exist in a α-PbO_2 structure type with no transformations, recent work has suggested otherwise. In 1967, Newnham[63] first noted the possibility of an order-disorder transformation based on the diffraction patterns obtained by Coughanour and coworkers.[64] More recently, work by McHale and Roth[65,66] has indicated this phase transformation, occurring at approximately 1100°C, as the cause for the change in the coefficient of thermal expansion between $ZrTiO_4$, the high temperature phase, and $ZrTi_2O_6$, proposed as a stable low temperature phase in the TiO_2-ZrO_2 system. However, despite recent interest in $ZrTiO_4$, other workers,[60,61] while acknowledging the presence of a low temperature polymorph, have not identified a phase of separate composition. Obviously, the presence of any phase transformation is less than ideal if $ZrTiO_4$ is to be developed as a potential coating material.

Several investigations have also revealed the thermal expansion coefficient of $HfTiO_4$ to be quite low.[55,57,59,60] Unlike $ZrTiO_4$, its α-PbO_2 structure is free of transformations.[59,60,67] This would provide a significant advantage over the destructive phase transformation experienced by HfO_2. Having a stable crystal structure, $HfTiO_4$ would not require stabilizers which could be leached out of the structure. Two important drawbacks exist, however, for $HfTiO_4$.[68] Although its CTE is low, it is highly anisotropic. As in the case of Al_2TiO_5, this could lead to significant microcracking and overall failure of the coating. Hf is also a rare and very expensive element, making the costs of producing a coating from this material a potentially limiting factor.

Much less is known about $Ta_2O_5 \cdot 6ZrO_2$ and $Ta_2O_5 \cdot 6HfO_2$. Both materials are reported[55,57] to have low thermal expansion coefficients and each has potential for good corrosion resistance, making them promising candidates. The lack of knowledge of these materials, as well as the possible complexity in obtaining exact stoichiometries

for $Ta_2O_5 \cdot 6ZrO_2$ and $Ta_2O_5 \cdot 6HfO_2$ and avoiding the production of homologous phases, pose potential problems concerning the ease with which they may be deposited.

On the other hand, the ease with which Ta_2O_5 can be deposited has already been demonstrated.[41,42,69,70] Additionally, phase equilibria studies of the Ta_2O_5-Na_2O system have shown that no liquid phases are present below 1625°C.[43] Formation of either of the sodium tantalate phases at typical application temperatures that are 300 to 500°C below the liquidus temperature would seem unlikely.[71]

In order to protect SiC and Si_3N_4 components, the candidate coating must not only inhibit any reaction with corrosive products found in its operating environment, but it must also prevent the oxygen present in a combustion atmosphere from diffusing through the coating to the surface of the component, which will oxidize in the presence of oxygen. Since oxygen can diffuse through most oxides at a significant rate, another barrier to oxygen must be established. This can be provided by the native silica layer which coats silicon-based ceramics. Silica, as investigated by many workers, is the best known oxygen diffusion barrier at high temperatures,[72] and it should prevent oxidation of the component. However, if the silica layer should either react with or diffuse into the protective coating which is deposited on top of it, its effectiveness to stop oxygen penetration would likely be destroyed. Although phase equilibria for the system Ta_2O_5-SiO_2 does not appear to be well established, the available data show that no liquid phases exist below 1550°C.[40] As in the formation of any intermediate sodium tantalate phases, no solid state reactions are expected at temperatures 200 to 400°C below the liquidus temperature, allowing SiO_2 to serve as an effective barrier to oxygen. To ensure compatibility between the silica layer and the protective Ta_2O_5 coating, long-term testing will need to be performed.

Experimental Procedure

Chemical vapor deposition of Ta_2O_5 on SiC substrates has been performed using the experimental setup shown in Figure 3.2. This system is contained in a quartz tube which is sealed at both ends with stainless steel end caps. The substrate is heated inductively by heating a graphite susceptor with a radiofrequency generator. Corrected substrate temperatures in the range of 1000 to 1300°C are measured using an optical pyrometer by sighting through a window in the end cap. In the first stage of the reactor, chlorine gas is passed over tantalum metal in a chlorinator electrically heated to approximately 600°C, producing $TaCl_5$ via

$$2Ta + 5Cl_2 = 2TaCl_5.$$

The addition of O_2 through a separate inlet tube causes the gases to react at the substrate via

$$4TaCl_5 + 5O_2 = 2Ta_2O_5 + 10Cl_2$$

to produce an adherent Ta_2O_5 coating on the substrate.

Sets of experiments were statistically designed using a 2^n factorial method to efficiently find the optimal deposition conditions. X-ray diffraction (XRD) techniques were used to verify the composition of the coating. Coating morphology was characterized using scanning electron microscopy (SEM) and optical microscopy.

Coatings deposited by CVD underwent preliminary testing for corrosion by Na_2SO_4 using a solution of distilled water and Na_2SO_4. A drop of solution was applied to the top center face of a coated sample and dried in a drying oven, thus leaving only the salt on the coating. This was repeated until a Na_2SO_4 concentration of 10 to 20 mg/cm^2 was obtained. Corrosion testing was performed in a four inch diameter quartz

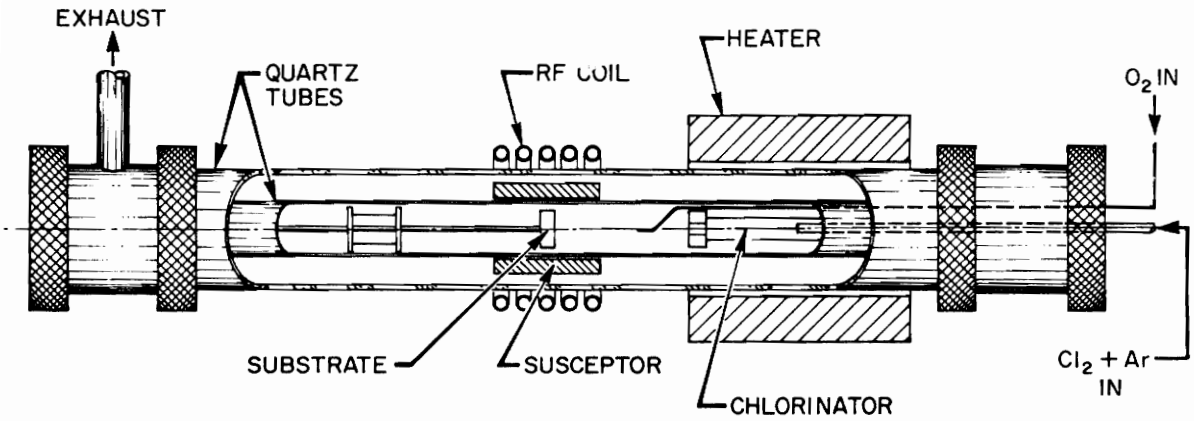

Figure 3.2: Schematic of CVD reactor

tube furnace at 1000°C for 100 hours with a 200 sccm flow of air passing over the specimens. Samples were then analyzed using XRD and SEM techniques.

Results and Discussion

The morphology of the Ta_2O_5 coating was strongly dependent on the deposition conditions. The statistically designed experiments examined the effects of system pressure, argon gas flow rate, substrate temperature, and oxygen and chlorine gas flow rates. Initial experiments over a range of substrate temperatures and gas flow rates indicated that regardless of substrate temperature or gas flow rates, consistently denser deposits of Ta_2O_5 were being formed at pressures of approximately 6.67 kPa (50 Torr) and using 40 sccm of argon to dilute the reactant gases. As a result, pressure and argon flow were fixed at these two values during the investigation. Gas flows for oxygen and chlorine ranged from 8 to 20 and 1 to 5 sccm, respectively.

Substrate temperatures of 1300°C produced coating structures which contained large, columnar grains with considerable intergranular passages. This structure can be seen in the optical and scanning electron microscope photographs shown in Figure 3.3. Obviously, this coating could do little to protect SiC or Si_3N_4 from the corrosive environment found in heat engines. Liquid Na_2SO_4 could flow in between the columnar grains with ease, attack and dissolve the SiO_2 coating the ceramic component, and subsequently attack the component itself.

Ta_2O_5 which was produced with high concentrations of reactants - an oxygen to chlorine to argon ratio of 10 to 3 to 40 - produced powders on the substrate surface. These can be seen in Figure 3.4. Even though most of the powders adhered to the substrate well enough to be examined by microscopy, it is certain that they would not be able to withstand the high pressure combustion environment, loaded with abrasive particulates, found in an engine.

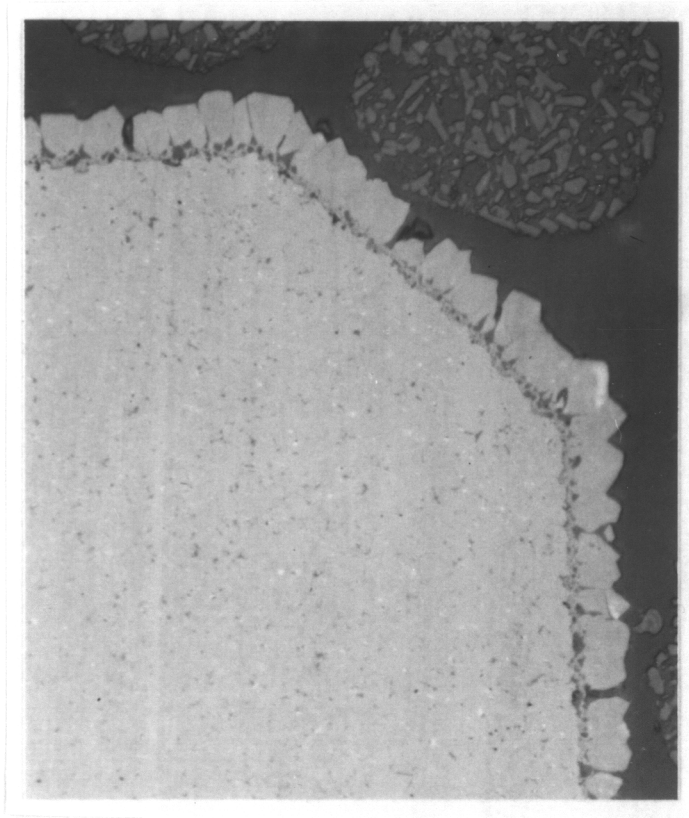

50 μm

(a) Photomicrograph of a section through the Ta_2O_5 coating and SiC substrate, as polished

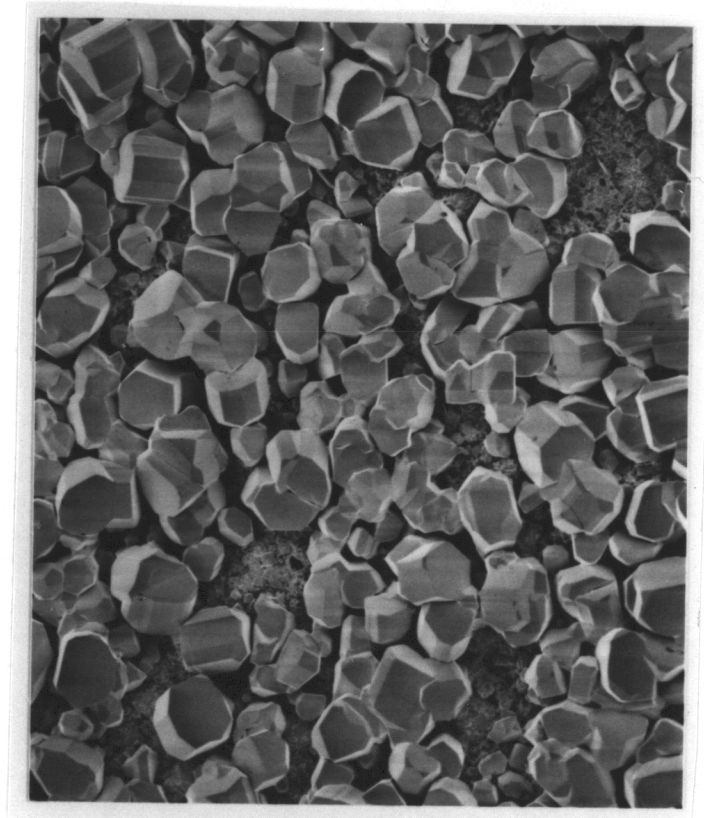

30 μm

(b) Scanning electron micrograph of the as-deposited Ta_2O_5 coating

Figure 3.3: Coating Morphology Produced by High Deposition Temperatures

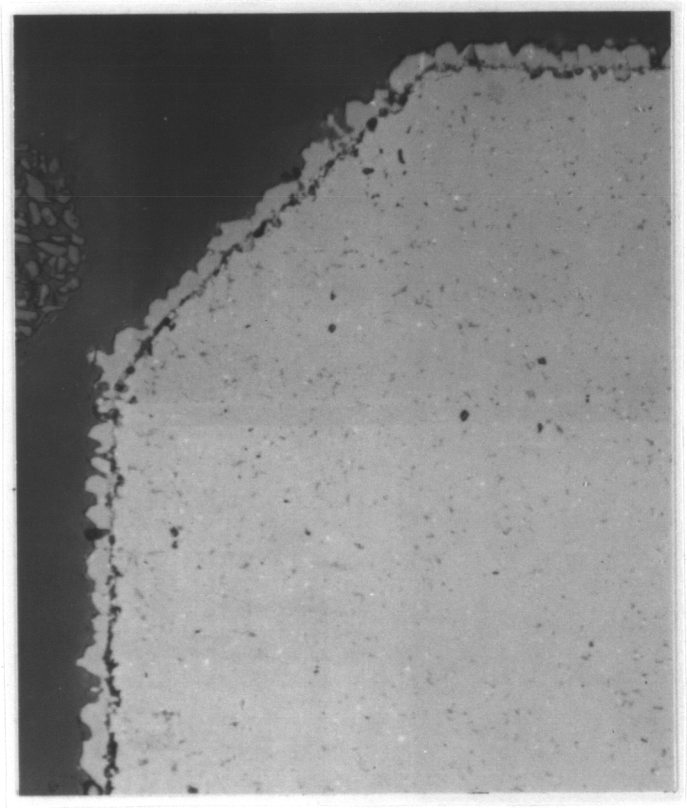

50 μm

(a) Photomicrograph of a section through the Ta_2O_5 coating and SiC substrate, as polished

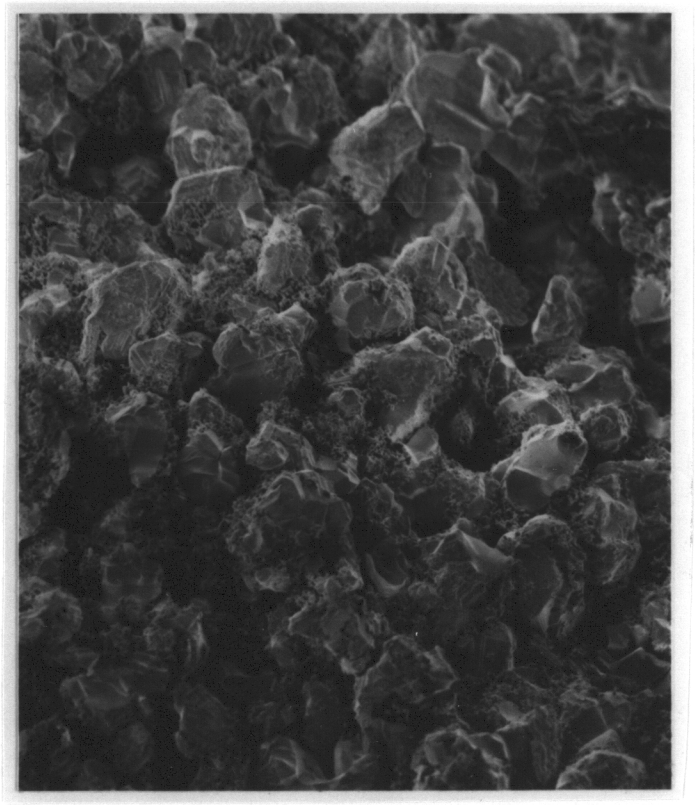

30 μm

(b) Scanning electron micrograph of the as-deposited Ta_2O_5 coating

Figure 3.4: Coating Morphology Produced by High Reactant Concentrations

At lower temperatures and with more dilute concentrations of reactant gases, more coherent coatings have consistently been produced which contain more equiaxed grains. As shown in Figure 3.5, these coatings are very uniform and continuous in structure. Unlike the morphologies described previously, they likely would not allow molten salts a direct path to the substrate surface.

Additional work is currently underway to further optimize coating morphology. The aim of refinements to the Ta_2O_5 structure is to produce finer, more equiaxed grains. Reducing grain size would decrease the diffusion path along grain boundaries to the substrate surface. If oxygen diffusion occurs along grain boundaries, a reduction in grain size would decrease the time required for oxygen transport across the coating. However, the protective silica coating which exists at the Ta_2O_5-coating interface would prevent the further oxidation of the component, rendering the issue of increased diffusion of oxygen irrelevant. Residual coating stresses due to anisotropy in the coefficient of thermal expansion would be minimized with a reduction in grain size. Coating morphologies such as these promise to protect the ceramic components in heat engines.

Preliminary corrosion tests using 15 mg/cm^2 of Na_2SO_4 in contact with CVD deposited Ta_2O_5 demonstrated that no apparent reaction occurred between the coating and the molten salt. As shown in the upper left corner of Figure 3.6, the Ta_2O_5 coatings which were tested consisted mainly of columnar grains and whiskers. Despite the coating morphology, no interaction of the coating or substrate with the molten salt seems to have taken place. An examination of Figure 3.6 indicates that the Na_2SO_4 in the lower right corner melted upon heating past its melting point and wetted the surface of the Ta_2O_5 coating. At the end of the corrosion test, the salt simply recrystallized as a polycrystalline film on the coating surface. These results were confirmed by X-ray diffraction, which identified SiC and Ta_2O_5 as the phases present. To more completely determine the suitability of Ta_2O_5 coatings, however, additional work is needed to test and subsequently analyze specimens under similar conditions for up to 1000 hours.

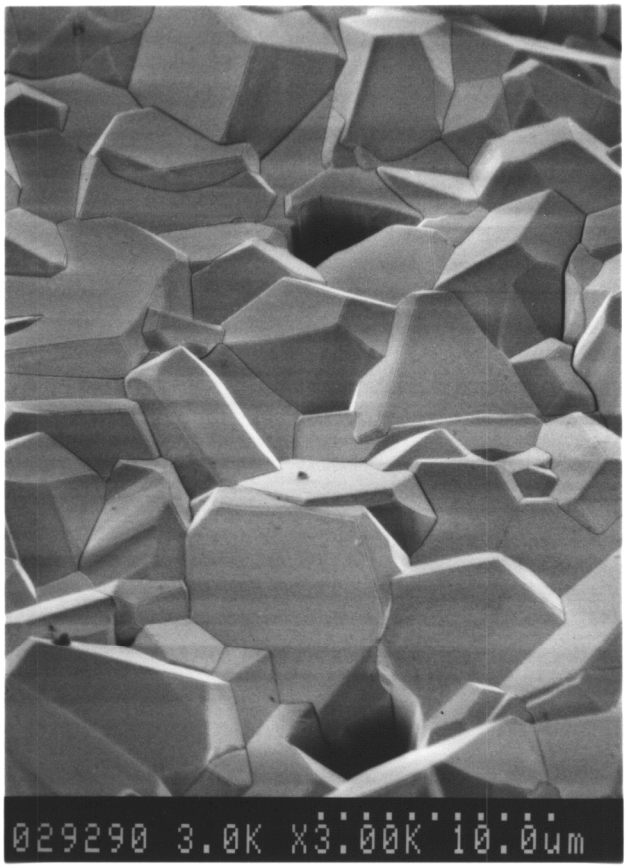

Figure 3.5: Scanning electron micrograph of coating produced using low deposition temperatures and low reactant concentrations

Figure 3.6: Scanning electron micrograph of the Ta_2O_5 and Na_2SO_4 interface after preliminary corrosion testing

Conclusions

SiC and Si_3N_4 heat engine components are susceptible to hot corrosion by molten Na_2SO_4 salts which are formed from impurities in the engine's fuel and air intake. A number of oxides have been identified which may protect these components from corrosion. Among these, Ta_2O_5 was selected as one of the most promising candidates, and chemical vapor deposition techniques have been developed to deposit it onto SiC substrates. Depending on the deposition conditions, a variety of coating morphologies have been produced, and conditions have been identified which produce dense, continuous Ta_2O_5 deposits. These conditions are being further optimized to produce a finer, more equiaxed microstructure. Additionally, preliminary corrosion tests with 15 mg/cm^2 of Na_2SO_4 at 1000°C showed no degradation of the CVD deposited coatings of Ta_2O_5.

CHAPTER 4: THERMODYNAMIC CONSIDERATIONS FOR THE CHEMICAL VAPOR DEPOSITION OF $ZrTiO_4$ USING CHLORIDE PRECURSORS

Introduction

Silicon carbide and silicon nitride materials have undergone extensive development in recent years for use in a wide variety of applications such as heat exchangers, hot gas cleanup systems, and advanced heat engines. In these types of systems, ceramics will be susceptible to hot corrosion in the form of attack by molten salts such as Na_2SO_4 formed from NaCl present in the atmosphere and sulfur impurities in the fuel.[30] Long term exposure to these types of conditions has been shown to degrade the properties of structural ceramics.[17,19,25,27,30]

Exposed surfaces of silicon-based ceramics oxidize at high temperatures to form a layer of silica which serves to inhibit further oxidation of the ceramic.[32] This silica layer can react with the molten salt to form a sodium-silicate liquid phase at temperatures above approximately 800°C,[19-21,33] the eutectic temperature in the sodium-silica system.[47] As a result, the ceramic loses its protective layer and degradation of the material occurs.[20,21,27]

Due to the nature of the service conditions under which these ceramic components

are expected to perform, it becomes necessary to use a coating for corrosion protection. The selection criteria for a protective coating have been established. The first and most obvious coating requirement is the ability of the coating to resist reaction with an aggressive salt layer. It must also have a coefficient of thermal expansion (CTE) that is very close to that of SiC and Si_3N_4. This requirement would minimize noncatastrophic cracking which could allow molten salt to penetrate the coating and result in a loss of corrosion protection. Closely matched CTE's would also overcome the problems with adherence which were experienced, for example, with the protective coating system developed at GTE Laboratories.[48-51] The coating material must also be a stable oxide to provide inherent oxidation resistance. Additionally, considerations for weight and cost must also be taken into account.

Coating materials that have been identified to protect SiC and Si_3N_4 components from salt-induced corrosion include mullite, Al_2TiO_5, Ta_2O_5, $ZrTiO_4$, $HfTiO_4$, $Ta_2O_5 \cdot 6ZrO_2$, and $Ta_2O_5 \cdot 6HfO_2$. These are currently being investigated for this purpose as well as for other applications.[53,55-57] In addition to the work performed on these materials, work is being initiated to study $ZrTiO_4$ as a potential coating material. A number of investigations have shown the CTE of $ZrTiO_4$ to be quite low.[55,57,59,60,61] While the data summarized by Levin and McMurdie[62] show that $ZrTiO_4$ is thought to exist in an α-PbO_2 structure type with no phase transformations, recent work has suggested otherwise. In 1967, Newnham[63] first noted the possibility of an order-disorder transformation based on the diffraction patterns obtained by Coughanour and coworkers.[64] More recently, work by McHale and Roth[65,66] has indicated this phase transformation, occurring at approximately 1100°C, as the cause for the change in the coefficient of thermal expansion between $ZrTiO_4$, the high temperature phase, and $ZrTi_2O_6$, proposed as a stable low temperature phase in the TiO_2-ZrO_2 system. However, despite recent interest in $ZrTiO_4$ for other applications, other workers,[60,61] while acknowledging the presence of a low temperature polymorph, have not identified a phase of separate composition. However, they have noted the difference in CTE

between furnace cooled and quenched samples of $ZrTiO_4$ prepared at identical temperatures. Although their work was not conclusive, the difference in CTE may indicate metastability of the high temperature phase, which may allow the use of $ZrTiO_4$ in a variety of applications.

In the present study, the thermodynamics of the deposition of $ZrTiO_4$ by reaction of O_2 with titanium chloride and zirconium chloride is analyzed. In order to gain an understanding of any CVD process, it is well known that knowledge of the thermodynamics, kinetics, mass transport, and nucleation and growth must all be integrated in order to form a complete picture of the deposition process. With the lack of any prior work on $ZrTiO_4$, equilibrium calculations can provide a first step in determining thermodynamic limitations and can be used as a guide in determining suitable experimental conditions.

Thermochemical Data

The ChemSage computer program[12] was used to calculate chemical equilibria for the Zr-Ti-O-Cl system. This program uses numerical techniques to minimize the total Gibbs free energy of all of the possible gaseous, liquid, and solid species which may be present in a particular chemical system. As with all computer programs, the results which may be obtained from these calculations are only as good as the data which are input into the routine. In thermochemical calculations, the accuracy of the results will depend upon two factors in particular: the inclusion and omission of chemical species for consideration in equilibrium calculations, and the accuracy of the thermodynamic data which are utilized for these calculations.

Accompanying the ChemSage program was the thermodynamic database developed by Scientific Group Thermodata Europe (SGTE)[13] and the Microtherm[14] databank management computer program. In the SGTE database, thermodynamic data

are compiled in terms of the standard enthalpy of formation, ΔH°_f, at 298.15K, the entropy S° at 298.15K, the standard enthalpy of transformation ΔH° for phase transitions, and the molar specific heat at constant pressure C_p. The data for heat capacity are expressed as a function of temperature T so that $C_p = a + bT + cT^2 + dT^{-2}$ where a, b, c, and d are constants and T is in Kelvin. In addition to supplying database management capabilities, the Microtherm program also provided for the computation of various thermodynamic quantities such as the standard free energy of formation, ΔG°_f.

Table 4.1 enumerates the standard free energies of formation of the chemical species considered in the Zr-Ti-O-Cl system at 298.15K and 1500K. Solid, liquid, and gaseous species are denoted with (s), (l), and (g), respectively; condensible species are noted with (c), indicating the presence of either a solid or liquid, depending on the temperature. These values were calculated from thermodynamic data by the Microtherm program. To ensure the accuracy and integrity of the data contained in the SGTE database, the values for ΔG°_f were compared to recent modifications in the JANAF Tables[15] as well as to data compiled by Barin[16]. Although minor variations in data were encountered, the overall agreement between the three databases was good. Only a few of the species had values of ΔG°_f which differed between the databases by more than 2 kJ/mole. The chemical equilibria for this system is expected to be insensitive to such minor variations due to the magnitude of the energies of formation of the compounds in this system which are expected to be stable.

Discrepancies did exist, however, which must be addressed. The data for anatase were markedly different between the SGTE database and the JANAF Tables. Values for ΔG°_f differed by 5.620 kJ/mole at 298.15K and 6.771 kJ/mole at 1500K. Barin's data, based on the JANAF Tables, reflected these discrepancies as well. Considering the close similarity in ΔG°_f for anatase and rutile TiO_2, thermochemical stability between these phases may be affected by this difference and should not be ignored. Thus the data for anatase were modified to reflect the more recent revisions made in the JANAF Tables. The data for Zr(g) differed by ~ 11 kJ/mole at 298.15K and ~ 12 kJ/mole at 1500K.

Table 4.1: Free Energy Values for the Chemical Species Considered in the Zr-Ti-O-Cl System

Species	$\Delta G^{\circ}_{f,298.15K}$ (kJ/mole)	$\Delta G^{\circ}_{f,1500K}$ (kJ/mole)	Reference
Cl(g)	105.311	35.503	13
ClO(g)	97.479	81.619	13
TiClO(s)	-714.562	-	13
TiClO(g)	-249.901	-264.931	13
ClO_2(g)	122.308	193.938	13
TiCl(g)	122.494	1.697	13
ZrCl(g)	174.503	62.670	13
Cl_2(g)	0.000	0.000	13
Cl_2O(g)	105.044	172.572	13
$TiCl_2O$(g)	-535.049	-488.252	13
$TiCl_2$(s)	-465.897	-280.591	13
$TiCl_2$(g)	-244.575	-267.703	13
$ZrCl_2$(c)	-385.665	-233.420	13
$ZrCl_2$(g)	-195.286	-225.534	13
$TiCl_3$(s)	-654.555	-405.519	13
$TiCl_3$(g)	-524.903	-463.582	13
$ZrCl_3$(s)	-646.350	-398.071	13
$ZrCl_3$(g)	-514.054	-470.071	13
$TiCl_4$(l)	-733.914	-519.046	13
$TiCl_4$(g)	-726.848	-581.636	13
$ZrCl_4$(s)	-890.040	-	13
$ZrCl_4$(g)	-835.009	-696.727	13
O(g)	231.752	154.923	13
α-TiO(s)	-510.400	-397.204	13
β-TiO(s)	-510.130	-400.906	13
TiO(g)	24.517	-83.657	13
ZrO(g)	32.983	-57.616	13
O_2(g)	0.000	0.000	13
TiO_2-Anatase (s)	-883.384	-667.932	15
TiO_2(g)	-312.695	-328.958	13
TiO_2-Rutile (c)	-889.474	-673.705	13
ZrO_2(c)	-1039.728	-814.926	13
ZrO_2(g)	-295.023	-319.158	13
O_3(g)	163.165	245.528	13
Ti_2O_3(c)	-1433.945	-1112.067	13
Ti_3O_5(c)	-2317.496	-1800.248	13
Ti_4O_7(c)	-3213.267	-2478.794	13
$ZrTiO_4$(s)	-1931.795	-1491.132	Estimated
Ti(c)	0.000	0.000	13
Ti(g)	428.207	257.175	13
Zr(c)	0.000	0.000	13
α-Zr(s)	0.000	0.783	13
β-Zr(s)	4.845	-0.017	13
Zr(g)	578.072	410.335	13

Because this species has such a low partial pressure for the temperature range of this study, the data were not modified. Included among the JANAF tables is a $TiCl_4$ solid phase. This specie was omitted from consideration, as $TiCl_4$ becomes a liquid at 249K, and its presence as a solid would be highly unstable in the temperature regime which is being studied. TiO was also included in both Barin and JANAF as a liquid phase. This specie was also omitted, as the melting point of TiO is 2023K, making it similarly unstable in the temperature range which is being studied.

Another source of concern involves the $ZrTi_2O_6$ phase reported be McHale and Roth.[65,66] As described previously, other investigators have not identified this phase in the ZrO_2-TiO_2 system. Because of this lack of supporting evidence, as well as the lack of any thermochemical data for this composition, $ZrTi_2O_6$ was not considered.

Despite the recent literature involving $ZrTiO_4$, no work has been found in which its thermodynamic properties have been investigated. As a result, its data needs to be estimated. C_p data for $ZrTiO_4$ were easily obtained as a result of Kopp's rule. Kopp's rule states that the heat capacity of a solid or liquid compound is equal to the sum of the heat capacities of its constituent elements in the solid or liquid states.[73] As a consequence of Kopp's rule, the entropies of solid and liquid compounds can be estimated from the additivity of the entropies of their constituent components in the solid or liquid states.[74] With good estimates for C_p and $S^\circ_{298.15K}$ having been obtained, a value for $\Delta H^\circ_{f,298.15K}$ must be determined. It has been suggested that a good estimate of the enthalpy of formation of a compound may be obtained by similarly adding the enthalpies of the components.[75,76] Using the data already contained in the SGTE database, the enthalpy of formation for $ZrTiO_4$ was initially estimated by adding together the existing data for ZrO_2 and rutile TiO_2. This value was then used as a starting point from which the value of ΔH°_f was modified to gain agreement with the incongruent melting point of $ZrTiO_4$ at ~2123K.[62] The resulting thermochemical data estimated for $ZrTiO_4$ are listed in Table 4.2.

Table 4.2: Thermochemical data estimated for $ZrTiO_4$

Quantity	ZrO_2	Rutile TiO_2	$ZrTiO_4$
$\Delta H^\circ_{f,298.15K}$ (kJ/mole)	-1097.463	-944.747	-2044.804
$\Delta S^\circ_{298.15K}$ (J K^{-1} $mole^{-1}$)	50.36	50.29	100.65

Temperature (K)	C_p data are in J K^{-1} $mole^{-1}$		
300	56.268	55.299	111.566
400	63.857	62.849	126.705
500	67.766	67.176	134.933
600	70.238	69.955	140.179
700	72.027	71.757	143.784
800	73.452	73.088	146.539
900	74.666	74.077	148.742
1000	75.748	74.853	150.601
1100	76.746	75.489	152.234
1200	77.685	76.029	153.713
1300	78.583	76.500	155.083
1400	79.452	76.921	156.373
1500	74.475	77.304	151.779

Thermochemical Stability of the Precursors

For CVD processes, the reactivity and volatility of reagents must be assessed in order to determine their transportability and chemical integrity as precursors at elevated temperatures. The need for this type of examination was demonstrated recently by Lee *et al.*,[44] discovering that understanding the decomposition characteristics of NH_3 was critical before the overall thermodynamics of the CVD of Si_3N_4 from SiF_4 and NH_3 could be correctly analyzed.

In the proposed reactor design, multiple reactions are required for the deposition of $ZrTiO_4$. In the first stage of the reactor, chlorine gas is separately passed over Zr and Ti sponge at elevated temperatures to produce $ZrCl_4$ and $TiCl_4$ gases, respectively. O_2 is then introduced into the reactor via a separate gas inlet. In the second stage of the reactor, the gases flow into the hot zone, and they react to deposit $ZrTiO_4$.

At atmospheric pressure, $ZrCl_4$ is a gas above 609K, as shown in Figure 4.1, and only at temperatures greater than 1400K does a minor amount of $ZrCl_3$ and Cl form. Figure 4.2 illustrates that $ZrCl_4$ retains its stability at reduced pressures as well. At 1.33 kPa (10 Torr) total pressure, $ZrCl_4$ is a gas above 503K. Even at 1500K, the partial pressures of $ZrCl_3$ and Cl are less than 1 Pa. $TiCl_4$, as shown in figures 4.3 and 4.4, is a gas above 370K. It is somewhat less stable than $ZrCl_4$. However, the mole fraction of decomposition products is less than 10^{-2} at 1500K. These results indicate that both $ZrCl_4$ and $TiCl_4$ should be suitable for use as precursors over a wide range of temperatures and pressures.

Zr-Ti-O-Cl System

Thermodynamic calculations can be used to explore ranges of input parameters for a CVD system which will produce a specific condensed phase at equilibrium. A

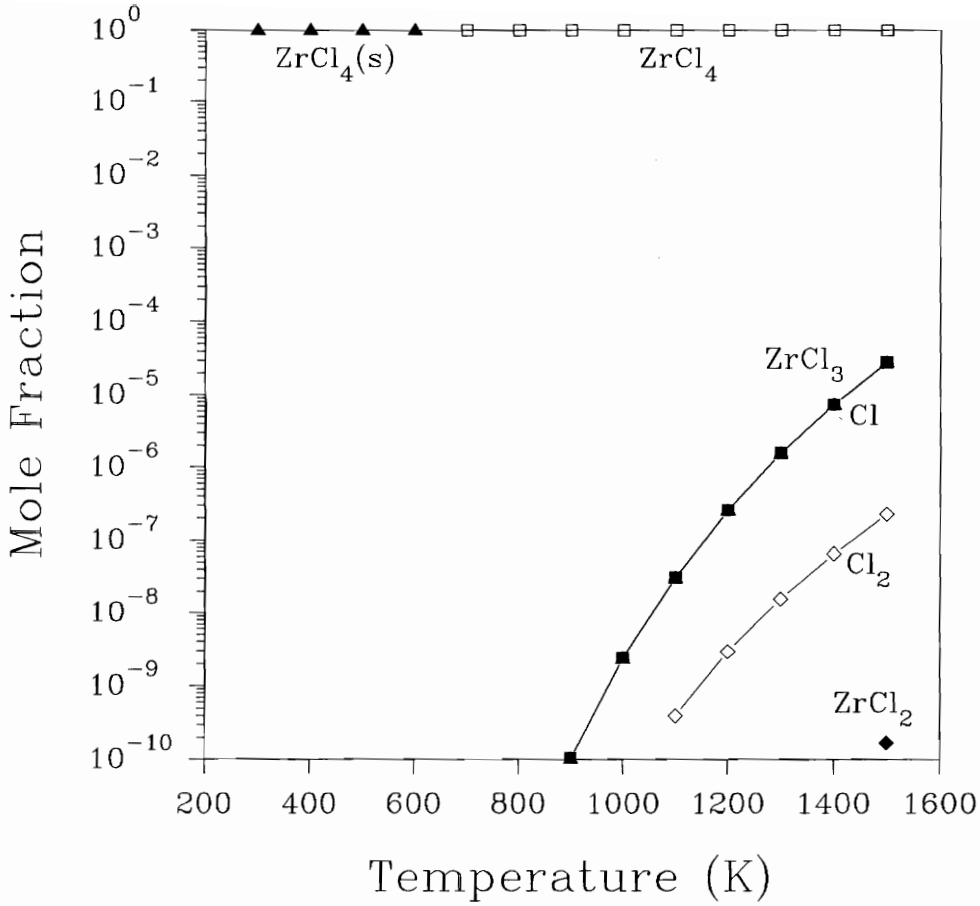

Figure 4.1: Equilibrium composition of one mole $ZrCl_4$ at 101 kPa

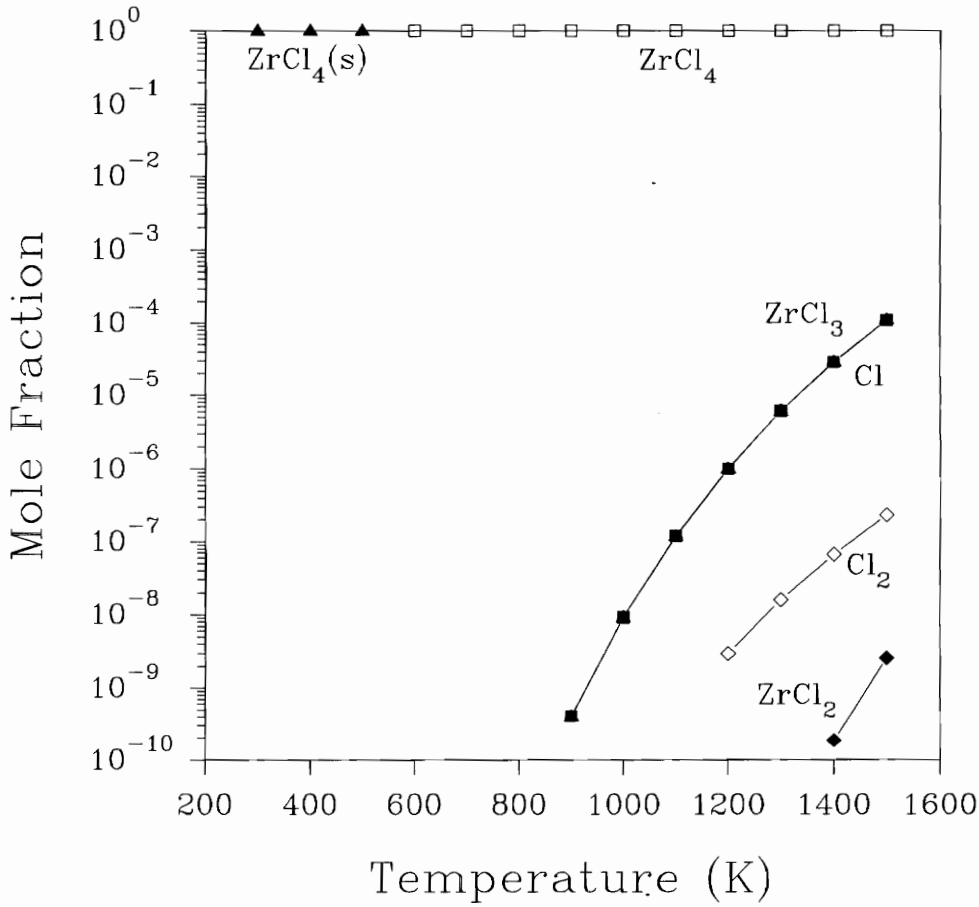

Figure 4.2: Equilibrium composition of one mole $ZrCl_4$ at 1.33 kPa

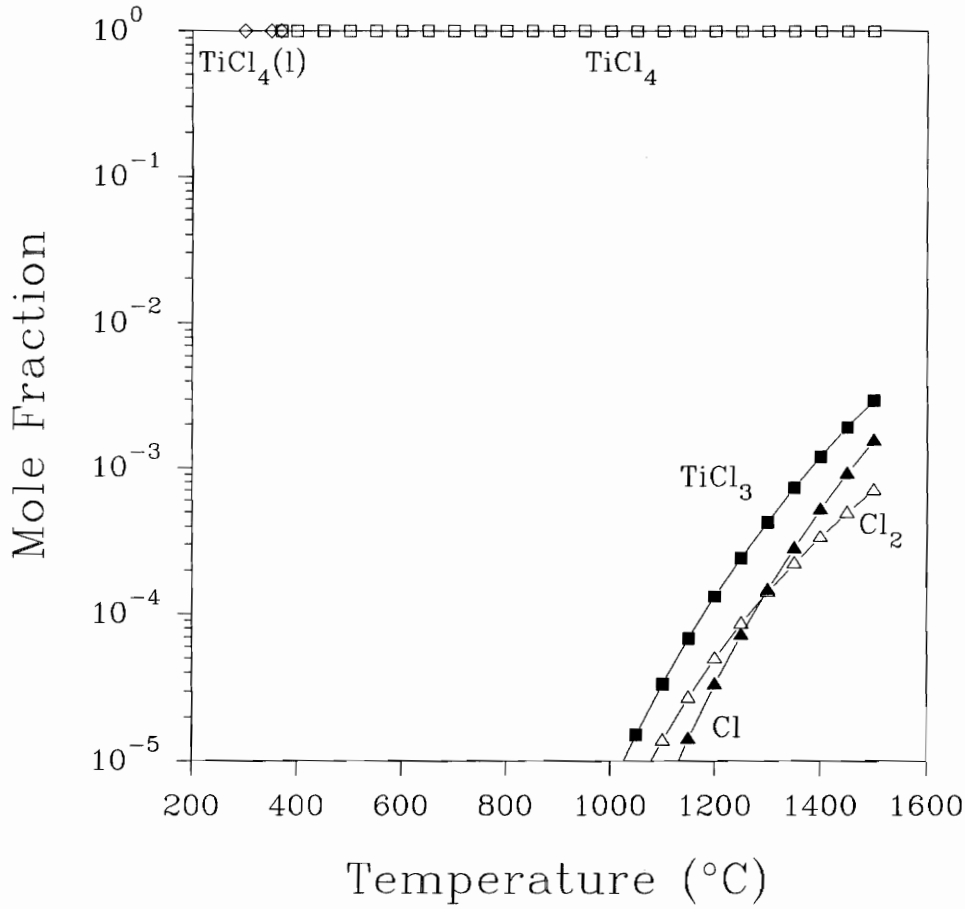

Figure 4.3: Equilibrium composition of one mole TiCl4 at 101 kPa

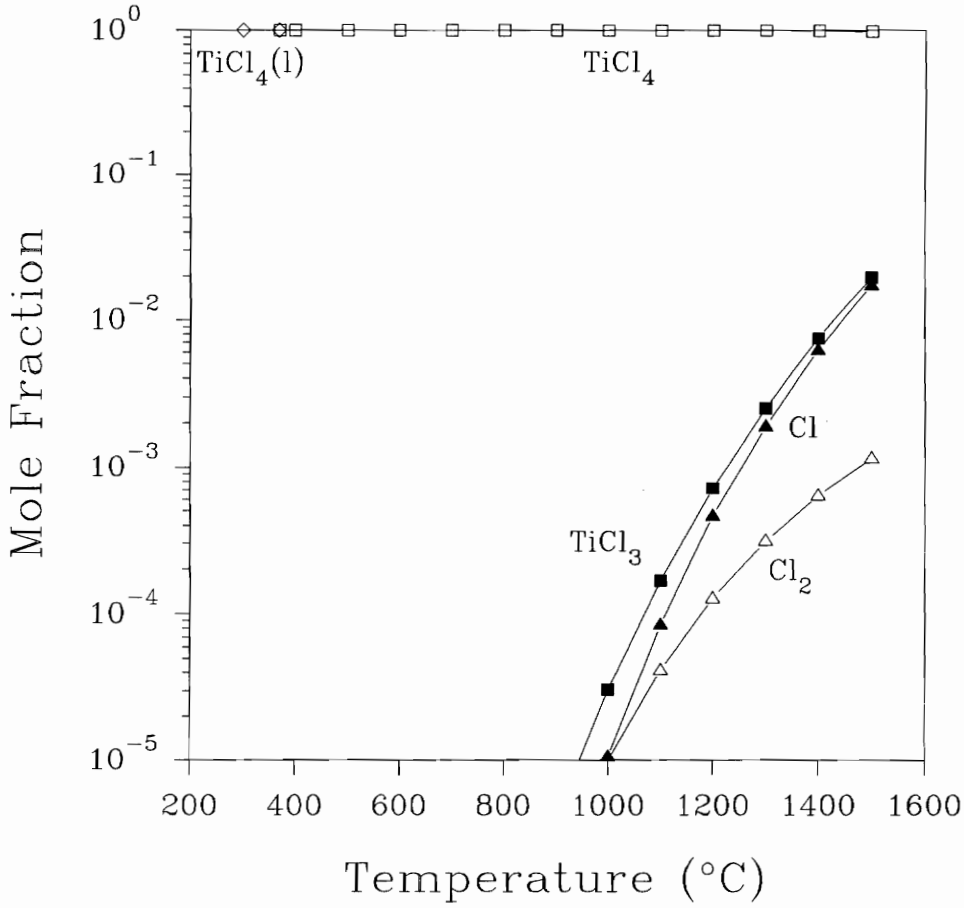

Figure 4.4: Equilibrium composition of one mole TiCl4 at 1.33 kPa

convenient method for displaying this information is the CVD phase diagram.[45,46] As in conventional phase diagrams, temperature, pressure, and composition may make up the axes which describe the parameters under consideration. These diagrams are plots of computed phase boundaries where the phase regions indicate the specific condensed phases which are the equilibrium products.

Figure 4.5 is a CVD phase diagram of the Zr-Ti-O-Cl system as a function of the reactant concentrations of $ZrCl_4$, $TiCl_4$, and O_2 at 1500K and 1.33 kPa. It can be seen in this diagram that $ZrTiO_4$ is thermodynamically favored to deposit as a single phase in only a very narrow region of the diagram. Figure 4.5 also illustrates that with increasing mole fraction of O_2, the codeposition of either ZrO_2 or TiO_2 with $ZrTiO_4$ becomes increasingly stable and the phase stability region for $ZrTiO_4$ narrows. ZrO_2 is predicted to be deposited as a single phase over a large portion of the $ZrCl_4$-rich region of the diagram. Finally, the deposition of TiO_2 as a single phase is predicted in the region of high concentrations of $TiCl_4$ and low concentrations of $ZrCl_4$.

CVD phase diagrams of the Zr-Ti-O-Cl system at 1.33 kPa and temperatures of 1173K and 1373K are essentially similar to the diagram produced at 1500K. As the temperature is increased from 1173K to 1500K, two effects can be noticed. First, the phase stability region for the single phase deposition of $ZrTiO_4$ widens to include a slightly larger range of $TiCl_4$ mole fractions. In addition, the range of $TiCl_4$ mole fractions at which $ZrTiO_4$ is deposited as a single phase shifts slightly towards the $ZrCl_4$-rich side of the diagram. At 1173K and a mole fraction of O_2 of 0.02, $ZrTiO_4$ is predicted to be deposited as a single phase when the $TiCl_4$ mole fraction is between 0.91 and 0.94. At 1500K, the range of $TiCl_4$ mole fractions shifts to include 0.84 to 0.88.

Conclusions

The results of the ChemSage calculations have indicated that the CVD of $ZrTiO_4$

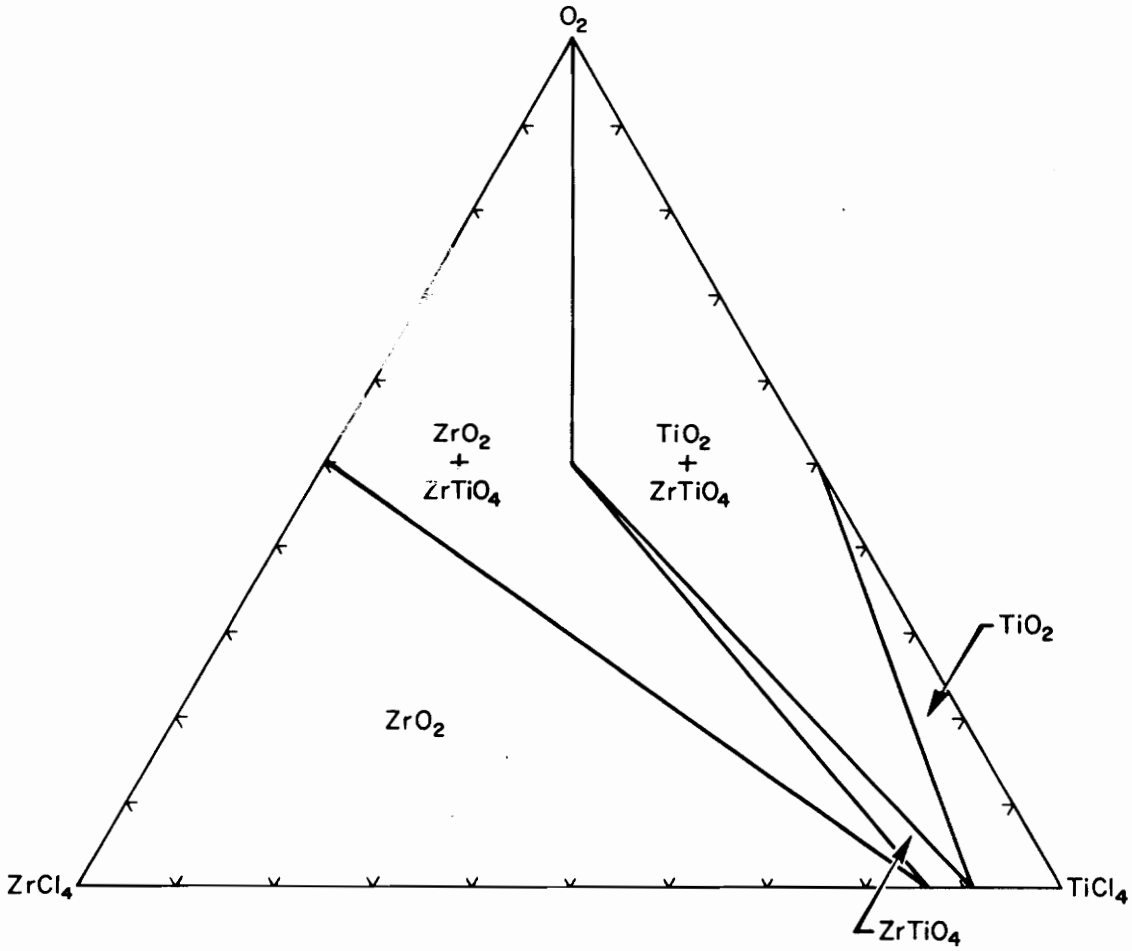

Figure 4.5: CVD phase diagram of the Zr-Ti-O-Cl system at 1500K and 1.33 kPa

from O_2, $ZrCl_4$, and $TiCl_4$ occurs over a range of temperatures in a narrow region of the phase diagram. Within the region of single phase deposition for $ZrTiO_4$, increases in the oxygen concentration causes phases other than $ZrTiO_4$ to become more stable. Substantial deviations in precursor concentrations outside of this phase region are likely to codeposit either ZrO_2 or TiO_2 with $ZrTiO_4$. As temperature is increased, the stability region for single phase deposition of $ZrTiO_4$ widens to include a slightly larger range of $TiCl_4$ mole fractions. In addition, the range of $TiCl_4$ mole fractions at which $ZrTiO_4$ is deposited as a single phase with increasing temperature shifts towards the $ZrCl_4$-rich side of the diagram.

Based on this work, the chemical vapor deposition of $ZrTiO_4$ is likely to be quite difficult. Very precise control and monitoring of the reactants will be required to insure that experimental conditions lie within the narrow region of single phase deposition. Even small variations from the target reactant composition will likely produce either TiO_2 or ZrO_2 as a second phase. Also, because $ZrTiO_4$ deposition occurs in a region of low oxygen concentrations, the production of zirconium titanate is very inefficient. Even in the region of single phase deposition, only a small fraction of the precursors would react to form the coating material, resulting in substantial amounts of unreacted chlorides.

CHAPTER 5: SUMMARY AND CONCLUSIONS

Silicon carbide and silicon nitride turbine engine components are susceptible to hot corrosion by molten sodium sulfate salts which are formed from impurities in the engine's fuel and air intake. Several oxide materials were identified which may be able to protect these components from corrosion. Despite the results of phase equilibria studies and thermochemical equilibrium calculations, the available information suggests that Ta_2O_5 coatings may be one of the most promising candidates. Thermochemical calculations showed that the chemical vapor deposition of tantalum oxide from O_2 and $TaCl_5$ precursors is thermodynamically feasible over a range of pressures, temperatures, and reactant concentrations. The deposition of Ta_2O_5 as a single phase is predicted in regions of excess oxygen, where the reaction is predicted to yield nearly 100% efficiency.

CVD experiments were carried out to deposit tantalum oxide films onto SiC substrates. Depending on the deposition conditions, a variety of coating morphologies have been produced, and conditions have been identified which produce dense, continuous Ta_2O_5 deposits. Preliminary corrosion tests on these coatings showed no apparent degradation of the CVD deposited tantalum oxide coatings.

The feasibility of depositing $ZrTiO_4$ as a coating material was also investigated based on thermochemical considerations. Since no data were available for this material, thermodynamic values were estimated. Thermochemical calculations indicated the

chemical vapor deposition of zirconium titanate from O_2, $ZrCl_4$, and $TiCl_4$ occurs over a range of temperatures in a very narrow region of the phase diagram. Deviations from the single phase region predicted the codeposition of either ZrO_2 or TiO_2 with $ZrTiO_4$. These results suggested that the chemical vapor deposition of $ZrTiO_4$ may be difficult from a process handling perspective. Additionally, the process is predicted to be very inefficient, leaving substantial amounts of unreacted chlorides in the reactor exhaust.

APPENDIX

Free Energy Values for the Chemical Species Considered in the Ta-O-Cl-Si-C-N-Na-S-H System

Species	$\Delta G^{\circ}_{f,298.15K}$ (kJ/mole)	$\Delta G^{\circ}_{f,1600K}$ (kJ/mole)	Reference
C(s)	0.000	0.000	13
C(g)	671.269	465.772	13
$C_{12}H_{26}$(g)	49.958	-	13
CCl(g)	470.107	328.837	13
CHCl(g)	319.113	255.521	13
CH_3Cl(g)	-60.195	67.949	13
CNCl(g)	130.998	96.334	13
COCl(g)	-76.528	-136.805	13
CCl_2(g)	227.580	177.683	13
CH_2Cl_2(g)	-68.974	62.873	13
$COCl_2$(g)	-205.940	-146.044	13
$CHCl_3$(g)	-70.409	75.800	13
CCl_3(g)	92.438	143.443	13
$SiCH_3Cl_3$(g)	-468.137	-	15
CCl_4(l)	-62.552	-	16
CCl_4(g)	-58.210	113.744	16
CH(g)	560.748	415.089	13
HCN(g)	124.709	82.422	13
HNCO(g)	-92.392	-45.536	13
HCO(g)	28.294	-30.396	13
CH_2(g)	369.230	302.182	13
H_2CO(g)	-109.900	-65.001	13
CH_2O_2(g)	-351.049	-	16
CH_3(g)	147.918	173.994	13
CH_4(g)	-50.818	85.838	13

$H_4CO(g)$	-162.514	-	13
$H_4CO(l)$	-166.351	-	13
CN(g)	404.995	273.373	13
NaCN(g)	67.324	2.699	13
NaCN(c)	-80.446	-14.079	13
NCO(g)	151.015	112.142	13
$CN_2(g)$	464.177	420.314	13
$Na_2CO_3(c)$	-1048.076	-647.116	13
CO(g)	-137.169	-252.254	13
COS(g)	-165.602	-217.679	13
$CO_2(g)$	-394.394	-396.376	13
α-SiC(s)	-69.115	-58.950	13
β-SiC(s)	-70.824	-61.317	13
cubic SiC(s)	-64.565	-47.578	13
SiC(g)	663.469	413.448	13
$Si_2C(g)$	476.265	230.329	13
CS(g)	228.837	72.462	13
$CS_2(l)$	65.102	58.308	13
$CS_2(g)$	66.833	-19.791	13
TaC(c)	-142.670	-140.591	13
$Ta_2C(s)$	-211.925	-209.073	13,16
$C_2(g)$	781.715	527.800	13
$C_2HCl(g)$	197.779	125.979	13
$C_2Cl_2(g)$	198.414	140.004	13
$C_2Cl_4(g)$	21.559	156.428	13
$C_2Cl_6(g)$	-56.855	280.376	16
$C_2H(g)$	438.016	270.338	13
$C_2H_2(g)$	209.168	137.730	13
$C_2H_3Cl(g)$	51.446	-	16
$C_2H_4(g)$	68.355	168.367	13
$C_2H_4O(g)$	-13.242	192.246	13
$C_2H_5Cl(g)$	-60.038	-	16
$C_2H_6(g)$	-32.928	239.039	13
CNC(g)	519.605	348.853	13
$(CN)_2(g)$	297.567	239.797	13
$(NaCN)_2(g)$	-21.071	20.227	13
$C_2O(g)$	251.105	91.641	13
$SiC_2(g)$	553.502	288.451	13
$C_3(g)$	754.448	477.274	13
$C_3H_4(g)$	202.347	-	13
$C_3H_6(g)$	104.164	-	13
$C_3H_8(g)$	-23.517	383.936	13
$C_3O_2(g)$	-109.703	-186.235	13
$C_4(g)$	909.429	638.607	13
$C_4H_{10}(g)$	-17.181	525.166	13

$C_4H_2(g)$	443.955	-	13
$C_4H_4(g)$	305.942	-	13
$C_4H_8(g)$	-69.220	-	13
$Si(CH_3)_4(g)$	-148.323	-	15
$C_4N_2(g)$	510.871	396.890	13
$C_5(g)$	915.422	632.467	13
$C_5H_{10}(g)$	38.565	-	13
$C_5H_8(g)$	110.761	-	13
$C_8H_6(g)$	361.719	-	13
$C_9H_{16}(g)$	243.711	-	13
$Cl(g)$	105.311	29.473	13
$HCl(g)$	-95.299	-104.376	13
$HOCl(g)$	-61.715	1.608	13
$SiH_3Cl(g)$	-119.359	-0.762	15
$NH_4Cl(c)$	-203.191	-	13
$NH_4ClO_4(s)$	-88.774	-	13
$NaCl(c)$	-384.047	-247.461	13
$NaCl(g)$	-201.325	-229.571	13
$NaClO_4(s)$	-254.325	-	15
$NOCl(g)$	66.078	127.694	13
$NO_2Cl(g)$	53.928	235.367	13
$ClO(g)$	97.479	80.257	13
$ClO_2(g)$	122.308	199.781	13
$SiCl(g)$	166.295	33.150	13
$SCl(g)$	128.534	71.157	13
$S_2Cl(g)$	43.840	25.341	13
$TaCl(g)$	328.126	-	16
$Cl_2(g)$	0.000	0.000	13
$SiH_2Cl_2(g)$	-294.934	-170.676	13
$Na_2Cl_2(g)$	-565.935	-457.911	13
$Cl_2O(g)$	105.044	178.077	13
$SCl_2(l)$	-28.520	-	15
$SOCl_2(g)$	-197.552	-	13
$SO_2Cl_2(g)$	-310.359	-56.865	13
$SiCl_2(g)$	-180.375	-225.437	13
$SCl_2(g)$	-25.475	5.966	13
$S_2Cl_2(l)$	-38.682	-	13
$S_2Cl_2(g)$	-28.672	-	13
$TaCl_2(g)$	-77.067	-	16
$SiHCl_3(g)$	-464.934	-324.552	13
$TaOCl_3(s)$	-802.696	-	13
$TaOCl_3(g)$	-748.381	-	13
$SiCl_3(g)$	-379.878	-334.035	13
$TaCl_3(s)$	-487.202	-230.301	13
$TaCl_3(g)$	-313.250	-	16

$SiCl_4$	-625.365	-	13
$SiCl_4(g)$	-622.819	-454.561	13
$TaCl_4(s)$	-619.581	-	13
$TaCl_4(g)$	-540.779	-	13
$TaCl_5(c)$	-746.536	-	13
$TaCl_5(g)$	-709.374	-482.235	13
H(g)	203.293	130.699	13
NaH(s)	-33.567	-	13
NaH(g)	102.935	68.667	13
NaOH(c)	-379.771	-179.192	13
NaOH(g)	-200.462	-156.885	13
NH(g)	370.565	344.556	13
HNO(g)	112.380	175.243	13
$HNO_2(g)$	-44.014	113.220	13
$HNO_3(g)$	-74.015	195.183	13
OH(g)	34.277	14.753	13
$HO_2(g)$	14.413	75.791	13
SiH(g)	342.724	204.229	13
HS(g)	110.056	50.642	13
$H_2(g)$	0.000	0.000	13
$(NaOH)_2(g)$	-568.390	-274.988	13
$NH_2(g)$	199.830	251.493	13
$N_2H_2(g)$	243.845	394.812	13
$H_2O(l)$	-237.190	-	13
$H_2O(g)$	-228.857	-158.708	13
$H_2O_2(g)$	-105.479	-	13
$H_2SO_4(l)$	-690.022	-	13
$H_2SO_4(g)$	-653.434	-229.208	13
$H_2S(g)$	-33.329	-10.483	13
$H_2S_2(g)$	-5.637	-	13
$NH_3(g)$	-16.399	132.245	13
$N_2H_4(l)$	149.343	-	15
$N_2H_4(g)$	159.166	458.331	13
$SiH_4(g)$	56.794	181.311	13
$Si_2H_6(s)$	126.154	-	13
$(NH_4)_2SO_4(s)$	-901.873	-	13
N(g)	455.562	373.026	13
NO(g)	86.598	70.153	13
$NO_2(g)$	51.241	133.763	13
$NaNO_2(c)$	-290.143	-	16
$NaNO_3(c)$	-367.073	-	16
$NO_3(g)$	116.085	311.170	13
SiN(g)	341.927	216.601	13
$Si_2N(g)$	360.812	209.444	13
SN(g)	235.514	179.347	13

TaN(c)	-226.601	-127.956	16
Ta_2N(c)	-245.204	-138.536	16
N_2(g)	0.000	0.000	13
N_2O(g)	104.161	199.512	13
N_2O_3(g)	139.429	383.220	13
N_2O_4(l)	97.411	-	13
N_2O_4(g)	97.716	476.464	13
N_2O_5(g)	117.896	566.118	15
N_3(g)	432.373	506.773	13
α-Si_3N_4(s)	-647.406	-216.743	15
Na(c)	0.000	0.000	15
Na(g)	77.301	0.567	13
NaO(g)	61.304	19.642	13
NaO_2(s)	-218.746	-24.134	13
NaS(c)	-189.741	-127.680	13
NaS_2(c)	-196.427	-	13
Na_2(g)	104.106	55.220	15
Na_2O(c)	-379.107	-143.400	13
Na_2O_2(c)	-449.664	-126.203	13
Na_2SO_3(c)	-1012.375	-493.443	16
Na_2SiO_3(c)	-1467.380	-994.917	13
Na_2SO_4(c)	-1269.313	-665.765	13
Na_2SO_4(g)	-974.496	-548.005	13
$Na_2Si_2O_5$(c)	-2319.213	-1645.576	13
Na_2S(c)	-354.551	-170.447	15,16
Na_2S_2(c)	-392.172	-	15
Na_2S_3(c)	-403.584	-	13
Na_2S_4(c)	-392.272	-	16
Na_4SiO_4(c)	-1968.675	-1232.530	13
O(g)	231.752	148.299	13
SiO(g)	-127.289	-235.338	13
SO(g)	-21.009	-66.461	13
S_2O(g)	-86.387	-80.890	13
TaO(g)	163.539	48.818	13
O_2(g)	0.000	0.000	13
SiO_2-cristobalite(c)	-854.804	-626.300	13
SiO_2(g)	-306.925	-308.477	13
SiO_2-quartz(c)	-856.478	-627.973	13
SO_2(g)	-300.126	-244.173	13
TaO_2(g)	-210.863	-244.162	13
O_3(g)	163.165	252.238	13
SO_3(g)	-371.035	-194.191	13
Ta_2O_5(c)	-1911.089	-1360.583	13
Si(c)	0.000	0.000	13
Si(g)	406.179	215.320	13

$SiTa_2(s)$	-126.615	-130.492	16
$Si_2(g)$	532.687	294.173	13
$Si_2Ta(s)$	-112.318	-82.920	16
$Si_3(g)$	572.961	314.158	13
$Si_3Ta_5(s)$	-339.766	-355.505	16
S(c)	0.000	0.000	15
S(g)	236.533	120.890	13
SiS(g)	54.437	-94.169	13
TaS(g)	459.577	298.895	16
$S_2(g)$	-79.612	-0.612	13
$SiS_2(c)$	-212.609	-105.870	13
$TaS_2(s)$	-344.940	-	16
$S_3(g)$	89.777	66.544	15
$S_4(g)$	91.382	116.558	15
$S_5(g)$	65.137	193.713	15
$S_6(g)$	53.699	224.244	15
$S_7(g)$	59.034	261.187	15
$S_8(g)$	48.579	322.288	15
Ta(c)	0.000	0.000	13
Ta(g)	739.164	556.410	13

REFERENCES

1. D. J. Godfrey, "The Use of Ceramics in High-Temperature Engineering," *Metals Mater.*, **2** [10] 305-11 (1968).

2. A. E. Pasto, "Current Research Issues in Silicon Nitride Structural Ceramics," *MRS Bulletin*, **12** [10-11] 73-78 (1987).

3. M. L. Torti, "Ceramics for Gas Turbines, Present and Future," Paper No. 740242 in *Automotive Engineering Congress*, Detroit, 1974.

4. S. Motojima, H. Yagi, and N. Iwamori, "Chemical Vapor Deposition of SiC and Some of Its Properties," *J. Mater. Sci. Lett.*, **5** 13-15 (1986).

5. H. E. Hintermann, "Exploitation of Wear and Corrosion Resistant CVD Coatings," *Tribology Inter.* **13** [6] 267-277 (1980).

6. H. Itoh, M. Gonda, and K. Sugiyama, "CVD of Corrosion-Resistant TiN and TiC Films to Inner Wall of Steel Tubes," *Surface Technology of Metals*, **35** [12] 590-4 (1984).

7. H. E. Hintermann, "Wear and Corrosion Protection by CVD and PVD Coatings," *Merallober.*, **35** [3] 213-7 (1981).

8. J. T. K. Clark *et al.*, "The Development of CVD Oxide Coatings for the Protection of Metal Surfaces," *Proc. 4th European Conf. on CVD*, Eindhoven, The Netherlands, May 31 - June 2, 1983.

9. J. R. Strife and J. E. Sheehan, "Ceramic Coatings for Carbon-Carbon

Composites," *Am. Ceram. Soc. Bull.*, **67** [2] 369-74 (1988).

10. D. W. McKee, "Oxidation Behavior and Protection of Carbon/Carbon Composites," *Carbon*, **25** [4] 551-7 (1987).

11. D. W. McKee, "Oxidation Protection of Carbon-Carbon Composites," pp. 81-95 in *Proc. 5th Anual Conf. on Composite Technology*. Edited by M. Genisio. Southern Illinois University, Carbondale, IL, (1988).

12. G. Eriksson and K. Hack, "ChemSage - A Computer Program for the Calculation of Complex Chemical Equilibria," *Metall. Trans. B*, **21B** 1013-23 (1990).

13. SGTE Solution and Pure Substances Database was supplied by the developers of the ChemSage program; GTT Gesellschaft fur Technische, Thermochemie und -physik mbH, Kaiserstrabe 100, 5120 Herzogenrath 3.

14. Microtherm Thermodynamic Databank System for Inorganic Substances was supplied by the developers of the ChemSage program; GTT Gesellschaft fur Technische, Thermochemie und -physik mbH, Kaiserstrabe 100, 5120 Herzogenrath 3.

15. JANAF Thermochemical Tables; Parts I and II, Third Edition, *J. Physical and Chemical Reference Data*, **14** (1985).

16. I. Barin, *Thermochemical Data of Pure Substances; Parts I and II*, VCH mbH, Weinheim, Germany, 1989.

17. J. I. Federer, "Corrosion of SiC Ceramics by Na_2SO_4," *Adv. Ceram. Mater.*, **3** [1] 56-61 (1988).

18. D. S. Fox, N. S. Jacobson, and J. L. Smialek, "Hot Corrosion of Silicon Carbide and Silicon Nitride at 1000°C," *Ceram. Trans.*, **10** 227-49 (1990).

19. N. S. Jacobson and D. S. Fox, "Molten-Salt Corrosion of Silicon Nitride: II, Sodium Sulfate," J. Am. Ceram. Soc., **71** [2] 139-48 (1988).

20. N. S. Jacobson and J. L. Smialek, "Hot Corrosion of Sintered α-SiC at 1000°C," *J. Am. Ceram. Soc.*, **68** [8] 432-39 (1985).

21. N. S. Jacobson, C. A. Stearns, and J. L. Smialek, "Burner Rig Corrosion of SiC at 1000°C," *Adv. Ceram. Mater.*, **1** [2] 154-61 (1986).

22. C. H. Henager, Jr. and R. H. Jones, "Molten Salt Corrosion of Hot-Pressed Si_3N_4/SiC-Reinforced Composites and Effects of Molten Salt Exposure on Slow Crack Growth of Hot-Pressed Si_3N_4," *Ceram. Trans.*, **10**, 197-210 (1990).

23. N. S. Jacobson, "Kinetics and Mechanism of Corrosion of SiC by Molten Salts," *J. Am. Ceram. Soc.*, **69** [1] 74-82 (1986).

24. N. S. Jacobson, "Sodium Sulfate: Deposition and Dissolution of Silica," *Oxidation of Metals*, **31** [1/2] 91-103 (1989).

25. N. S. Jacobson, J. L. Smialek, and D. S. Fox, "Molten Salt Corosion of SiC and Si_3N_4," pp. 99-136 in *Handbook of Ceramics and Compsites, Vol. 1: Synthesis and Properites*. Edited by N. P. Cheremisnoff, Dekker, New York, 1990.

26. D. W. McKee and D. Chatterji, "Corrosion of Silicon Carbide in Gases and Alkaline Melts," *J. Am. Ceram. Soc.*, **59** [9-10] 441-4 (1976).

27. J. L. Smialek and N. S. Jacobson, "Mechanism of Strength Degradation for Hot Corrosion of α-SiC," *J. Am. Ceram. Soc.*, **69** [10] 741-52 (1986).

28. J. J. Swab and G. L. Leatherman, "Effects of Hot Corrosion on the Room Temperature Strength of Structural Ceramics," U. S. Army Materials Technology Laboratory Rept. No. MTL TR 89-68. Watertown, MA, July 1989.

29. J. J. Swab and G. L. Leatherman, "Static Fatigue Behavior of Structural Ceramics in a Corrosive Environment," U. S. Army Materials Technology Laboratory Rept. No. MTL TR 90-32. Watertown, MA, June 1990.

30. J. J. Swab and G. L. Leatherman, "Static-Fatigue Life of Ce-TZP and Si_3N_4 in a Corrosive Environment," *J. Am. Ceram. Soc.*, **75** [3] 719-21 (1992).

31. J. J. Swab and G. L. Leatherman, "Strength of Structural Ceramics after Exposure to Sodium Sulfate," *J. Eur. Ceram. Soc.*, **5** [6] 333-40 (1989).

32. J. A. Costello and R. E. Tressler, "Oxidation Kinetics of Hot-Pressed and Sintered α-SiC," *J. Am. Ceram. Soc.*, **64** [6] 327-31 (1981).

33. D. S. Fox and N. S. Jacobson, "Molten-Salt Corosion of Silicon Nitride: I, Sodium Carbonate," *J. Am. Ceram. Soc.*, **71** [2] 128-38 (1988).

34. N. S. Jacobson, M. J. McNallan, and E. R. Kreidler, "High Temperature Reactions of Ceramics and Metals with Chlorine and Oxygen," pp. 381-92 in *High Temperature Science, Vol. 27.* Humana Press, 1990.

35. J. E. Marra, E. R. Kreidler, N. S. Jacobson, and D. S. Fox, "Reactions of Silicon-Based Ceramics in Mixed Oxidation Chlorination Environments," *J. Am. Ceram. Soc.*, **71** [12] 1067-73 (1988).

36. M. J. McNallan, S. Y. Ip, S. Y. Lee, and C. Park, "Corrosion of Silicon-Based Ceramics in Mixed Oxygen-Chlorine Environments," *Ceram. Trans.*, **10** 309-33 (1990).

37. T. Sato *et al.*, "Corrosion of Silicon Nitride Ceramics in Aqueous Hydrogen Chloride Solutions," *J. Am. Ceram. Soc.*, **71** [12] 1074-79 (1988).

38. M. Shimada and T. Sato, "Corrosion of Silicon Nitride Ceramics in HF and HCl Solutions," *Ceram. Trans.*, **10** 355-65 (1990).

39. S. Lin, "Mass Spectrometric Studies on High Temperature Reaction Between Hydrogen Chloride and Silica/Silicon," *J. Electrochem. Soc.*, **123** [4] 512-14 (1976).

40. E. M. Levin and H. F. McMurdie, p. 167 in *Phase Diagrams for Ceramists, 1975 Supplement*, American Ceramic Society, Westerville, OH, 1975.

41. T. Takahashi and H. Itoh, "Formation of Tantalum Oxide by Chemical Vapor Deposition," *J. Less-Common Metals*, **38** 211-19 (1972).

42. E. Kaplan, M. Balog, and D. Frohman-Bentchkowsky, "Chemical Vapor Deposition of Tantalum Pentoxide Films for Metal-Insulator-Semiconductor Devices," *J. Electrochem. Soc.: Solid State Science and Technology,* **123** [10] 1570-3 (1976).

43. E. M. Levin and H. F. McMurdie, p. 92 in *Phase Diagrams for Ceramists, 1975 Supplement*, American Ceramic Society, Westerville, OH, 1975.

44. W. Y. Lee, J. R. Strife, and R. D. Veltri, "Low-Pressure Chemical Vapor Deposition of α-Si_3N_4 from SiF_4 and NH_3: Kinetic Characteristics," *J. Am. Ceram. Soc.*, **75** [8] 2200-6 (1992).

45. K. E. Spear, "Applications of Phase Diagams and Thermodynamics to CVD," pp.

1-16 in *Proc. Seventh Int'l Conf. on Chemical Vapor Deposition*. Edited by T. O. Sedgwick and H. Lydtin. The Electrochemical Society, Princeton, NJ, 1979.

46. T. M. Besmann, "Applications of Thermochemical Modeling to Chemical Vapor Deposition Processes," pp. 311-25 in *Proc. First Int'l Conf. on Surface Modification Technology*. Edited by T. S. Sudarshan and D. G. Bhat. The Metallurgical Society, Phoenix, AZ, 1988.

47. E. M. Levin, C. R. Robbins, and H. F. McMurdie, p. 94 in *Phase Diagrams for Ceramists*, The American Ceramic Society, Westerville, OH, 1964.

48. V. K. Sarin, "Design Criteria for a Coating to Reduce Contact Stress Damage," in *Proceedings of the DOE Workshop on Coatings for Advanced Heat Engines*, Castine, ME, July 1987.

49. S. F. Wayne, J. H. Selverian, and D. O'Neil, "Development of Adherent Ceramic Coatings to Reduce Contact Stress Damage of Ceramics: Final Report - Phase II," GTE Laboraories Inc., Waltham, MA, July 1992.

50. H. E. Rebenne and V. K. Sarin, "Ceramic Coatings to Reduce Contact Stress Damage of Ceramics - Thermodynamic Modeling," pp. 199-206 in *Proceedings of the 25th Automotive Technology Development Contractors' Coordination Meeting*, Society of Automotive Engineers, P-209, Warrendale, PA, 1988.

51. H. E. Rebenne and J. H. Selverian, "Adherent Ceramic Coatings to Reduce Contact Stress Damage of Ceramics," pp. 227-38 in *Proceedings of the Annual Automotive Technology Development Contractors' Coordination Meeting*, Society of Automotive Engineers, P-243, Warrendale, PA, 1991.

52. N. J. Shaw *et al.*, "Materials for Engine Applications Above 3000°F - an Overview," NASA Technical Memorandum 100169. NASA-Lewis Research Center, Cleveland, OH, Oct. 1987.

53. J. W. McCoy, "Long-Term Oxidation Protection of Carbon-Carbon Flight Structures," Wright Laboratory Rept. No. WL-TR-91-4091. Wright-Patterson Air Force Base, OH, March 1992.

54. J. W. McCoy, "Oxide-Based Overcoating of Carbon-Carbon," pp. 660-702 in *1990 Oxidation Resistant Carbon-Carbon Programs Review*, Wright Research and Development Center, Wright-Patterson Air Force Base, OH, November 1990.

55. I. Y. Glatter, D. J. Treacy, J. E. Sheehan, and K. S. Mazdiyasni, "High-Temperature Chemical Behavior of a Multi-Layered Oxidation Protection Coating System for Carbon-Carbon Composites," Wright Research and Development Center, Rept. No. WRDC-TR-89-4127. Wright-Patterson Air Force Base, OH, December 1989.

56. M. A. Alvin, D. M. Bachovchin, J. E. Lane, and R. E. Tressler, "Degradation of Cross Flow Filter Material," pp.162-7 in *Proceedings of the Seventh Annual Coal-Fueled Heat Engines and Gas Stream Cleanup Systems Contractors' Review Meeting*, Rept. No. DOE/METC-90/6110. Edited by H. A. Webb, *et al.*, U. S. Dept. of Energy, Morgantown, WV, 1990.

57. M. Milosevski, *et al.*, "Influence of Some Oxides on the Thermal Expansion Characteristics of Al_2TiO_5," *Proceedings of the 4th International Symposium on Ceramic Materials and Components for Engines*, to be published.

58. F. J. Parker, "Al_2TiO_5-$ZrTiO_4$-ZrO_2 Composites: A New Family of Low-Thermal-Expansion Ceramics," *J. Am. Ceram. Soc.*, **73** [4] 929-32 (1990).

59. R. Ruh, G. W. Hollenberg, E. G. Charles, and V. A. Patel, "Phase Relations and Thermal Expansion in the System HfO_2-TiO_2," *J. Am. Ceram. Soc.*, **59** [11-12] 495-9 (1976).

60. H. Ikawa *et al.*, "Phase Transformation and Thermal Expansion of Zirconium and Hafnium Titanates and Their Solid Solutions," *J. Am. Ceram. Soc.*, **71** [2] 120-7 (1988).

61. H. Ikawa, H. Shimojima, K.Urabe, and O. Fukunaga, "Thermal Expansion of Solid Solutions in the $ZrTiO_4$-In_2O_3-M_2O_5 (M = Sb,Ta) System," *J. Am. Ceram. Soc.*, **74** [8] 1899-904 (1991).

62. E. M. Levin and H. F. McMurdie, p. 169 in *Phase Diagrams for Ceramists, 1975 Supplement*, American Ceramic Society, Westerville, OH, 1975.

63. R. E. Newnham, "Crystal Structure of $ZrTiO_4$," *J. Am. Ceram. Soc.*, **50** [4] 216 (1967).

64. L. W. Coughanour, R. S. Roth, and V. A. DeProsse, "Phase Equilibrium Relations in the Systems Lime-Titania and Zirconia-Titania," *J. Res. Nat. Bur. Std.*, **52** [1] 37-42 (1954).

65. A. E. McHale and R. S. Roth, "Low-Temperature Phase Relationships in the System ZrO_2-TiO_2," *J. Am. Ceram. Soc.*, **69** [11] 827-32 (1986).

66. A. E. McHale and R. S. Roth, "Investigation of the Phase Transition in $ZrTiO_4$ and $ZrTiO_4$-SnO_2 Solid Solutions," *J. Am. Ceram. Soc.*, **66** [2] C-18-C-20 (1983).

67. K. S. Mazdiyasni and L. M. Brown, "Preparation and Characterization of High-Purity $HfTiO_4$," *J. Am. Ceram. Soc.*, **53** [11] 585-9 (1970).

68. G. Bayer, M. Hofmann, and L. J. Gauckler, "Effect of Ionic Substitution on the Thermal Expansion of $ZrTiO_4$," *J. Am. Ceram. Soc.*, **74** [9] 2205-208 (1991)

69. K. Hieber and M. Stolz, "Preparation of CVD Molybdenum, Tantalum, and Tantalum Oxide Layers," pp. 436-49 in *Proceedings of the Fifth International Conference on Chemical Vapor Deposition*. Edited by J. M. Blocher, H. E. Hintermann, and L. H. Hall. Electrochemical Society, Princeton, 1975.

70. M. Tsubuya *et al.*, "Manufacturing Method of Tantalum Oxide Film," *Japanese Kokai Patent Application No. Hei 3[1991]-284846*, Dec. 16, 1991.

71. D. W. Richerson, pp. 113 and 116-8 in *Modern Ceramic Engineering, Second Edition*, Dekker, New York, 1992.

72. I. Bush, C. Schmidt, and R. Tomashot, Editors, *Proceedings of the Air Force Workshop on Oxidation Protected Carbon-Carbon Composites (Below 3000°F)*, Air Force Wright Aeronautical Laboratories Final Report No. AFWAL-TR-88-4071. Wright-Patterson Air Force Base, OH, March 1988.

73. H. Kopp, *Ann. Chem. Pharm. Suppl.*, **3** [1] 289 (1864).

74. C. H. P. Lupis, *Chemical Thermodynamics of Materials*, North-Holland, New York, 1983.

75. T. M. Besmann, Oak Ridge National Laboratory, personal communication.

76. B. Gallois, Stevens Institute of Technology, personal communication.

VITA

David W. Graham was born on October 12, 1968 in Monterey, California. He trounced around the world as an Army brat unitl he settled down in Roanoke, Virginia in 1980 when his father retired from the service. After completing high school in Roanoke, he attended Virginia Tech as an undergraduate and in 1991 he received his bachelor of science in materials engineering. He then continued his education in graduate school at Virginia Tech through a joint effort with Oak Ridge National Laboratory.